Dear Editor,

We thank the Reviewers for their thoughtful and thorough review of our manuscript. We appreciate the time and effort that they put into the reviews and we think that their comments have greatly improved our paper. We hope that we have sufficiently addressed the reviewer comments.

We have made substantial changes to the manuscript (please see detailed responses below), but the core of our paper has not changed and the emissions corrections suggested by the Reviewers have slightly improved the agreement with the City of Boulder results. We have modified the Introduction to incorporate the additional references suggested by the reviewers, as well as shorten it. We have added some additional details about the performance of the dual-comb spectrometer, based our previous work, and included a new figure of the Allan deviations. We have modified the Results and Discussion primarily to include additional uncertainty analysis and to incorporate a more thorough analysis of the non-CO_2 sources. We have updated Figure 1 and (now) 7 to incorporate reviewer comments including showing the footprints of the two paths based on a STILT-R calculation.

We have further made numerous small changes to the text and minor changes to all figures, such as making axes larger, to improve readability.

The reviewer comments are reproduced below in black. Our responses are below the reviewer comments in blue and italics. Our changes to the main text are in green. All line numbers refer to the clean version revised paper.

Sincerely,

Eleanor Waxman on behalf of the authors

Responses to specific reviewer comments:

Reviewer 1:

The open-path dual-comb spectrometer measurements are novel and could be of interest to numerous urban greenhouse gas (GHG) researchers. However, I see two major problems that preclude this paper from being publishable.

My major criticisms of the paper fall into two main categories: 1) Quality of measurements For a relatively new measurement technique, the paper is lacking in demonstration of measurement quality. Can these measurements be compared against nearby in-situ CO_2 observations? I believe the National Center for Atmospheric Research is carrying out CO_2 measurements on one of its buildings in Boulder (PI: Britton B. Stephens). NOAA-Earth System Research Laboratory (just next door to NIST, where the authors are based) is the world leader for in-situ CO_2 measurements, managing a wide network of CO_2 measurement sites. Perhaps there are suitable measurement sites managed by NOAA-ESRL (e.g., a nearby tall tower) that can be used to compare against the horizontal column measurements shown in this paper?

We have previously published work demonstrating the measurement quality of the DCS and apologize for not appropriately reviewing these results in this manuscript. In particular, we did the suggested comparison in a previously published work, Waxman et al. (2017) AMT. In addition to comparing two different DCS systems, we further compared them to a point sensor CRDS instrument (Picarro) measuring CO_2 and CH_4 whose inlet was located at approximately the midpoint of the path. This instrument was calibrated by NOAA GMD immediately after completing the measurement campaign discussed in this work. Note that in this comparison, we carefully located the point sensor along our "reference" measurement path. We think that this is an even better comparison than to the point sensor at NCAR, which is further away. Similarly, the nearest tall tower in operation during this campaign was the Boulder Atmospheric Observatory in Erie, Colorado which is approximately 22 km to the northeast of NIST in the middle of oil and gas fields. Due to the distance between the tall tower and our measurements, any comparison would have much larger uncertainty than the one already conducted in Waxman et al. (2017).

At lines 119-136, we have modified the text to say:

In previous work (Waxman et al., 2017), we confirmed the high precision and accuracy possible with open-path DCS. Two DCS instruments, constructed by different teams, measured atmospheric air over adjacent paths over a two-week period. The retrieved path-averaged gas concentrations agreed to better than 0.6 ppm (0.14%) for CO_2 and 7 ppb (0.35%) for CH_4 across the full two week period, where the analysis of the two DCS instruments used a common spectral database (HITRAN 2008, Rothman et al., 2009) to retrieve the concentrations from the absorption spectrum. In the work here, a single DCS instrument probes the concentrations across two different open paths simultaneously, which should further suppress any systematic offsets to below 0.45 ppm (Waxman et al., 2017). In addition, (Waxman et al., 2017) compared the two DCS instruments to a stationary cavity ringdown (CRDS) point sensor whose inlet was approximately at the midpoint of the open path. This comparison actually took place over the reference path during the first two weeks of the present work. During that time, we found a roughly constant difference of 3.4 ppm CO_2 and 17 ppb CH_4 between the DCS and CRDS systems. At present, we attribute this offset to differences in the calibration scheme as the DCS is tied to the HITRAN database while the CRDS is tied to the manometric (or gravimetric

depending on the gas) WMO scale. Similar level offsets have been observed in comparison of the TCCON open-path FTS instrument and point sensor-based vertical columns resulting in the TCCON CO_2 scaling factor of 0.9898 (4.08 ppm for a mixing ratio of 400 ppm) (Wunch et al., 2017). This offset does not affect the results here as it is common to both the reference and over-city paths.

The observational time series shown in Fig. 6 is quite noisy, it appears. The authors claim that the noise in the XCO2 reference path is associated with wind gusts of clean air, but no evidence is shown for this claim. Moreover, if the noise is due to gusts of clean air, why are there no such patterns showing up in the XCH4 time series? It is also concerning that the Q(t) time series does not appear to indicate a peak during the rush hour even on a weekday (10/25/2016).

Figure 6 originally showed data at 30 second time resolution. There was no particular reason to show the data at this fine a time resolution and it adds white noise. We have updated the figure (now Figure 7) and all other figures to show data smoothed to 5 minute time resolution. In addition, we have further modified the axis range for the CO_2 on Oct. 22 to cover the same range as the Oct. 25 data and have removed the CH_4 time series as it is not relevant to the emissions analysis and Q(t) calculation.

We have looked more closely at the data in the old Figure 6 and agree with the reviewer that it is unlikely to be due to gusts of clean air. We now include representative footprints for the reference and over-city paths generated from STILT. We ascribe the greater variability along the reference path (red traces in Fig. 7) to the smaller footprint for this path as seen in Fig. 7. If the air entering the city is not fully mixed the spatial and temporal variability will be much more evident in the reference path because of the smaller footprint. Thus this is in a sense a representation error due to the path location selection. There are no major sources or sinks of CH_4 west of Boulder as opposed to CO_2 so we expect the CH_4 to be more well-mixed than the CO_2 and thus we do not expect such patterns in the CH_4 timeseries.

The modified Figure 7 is reproduced below.

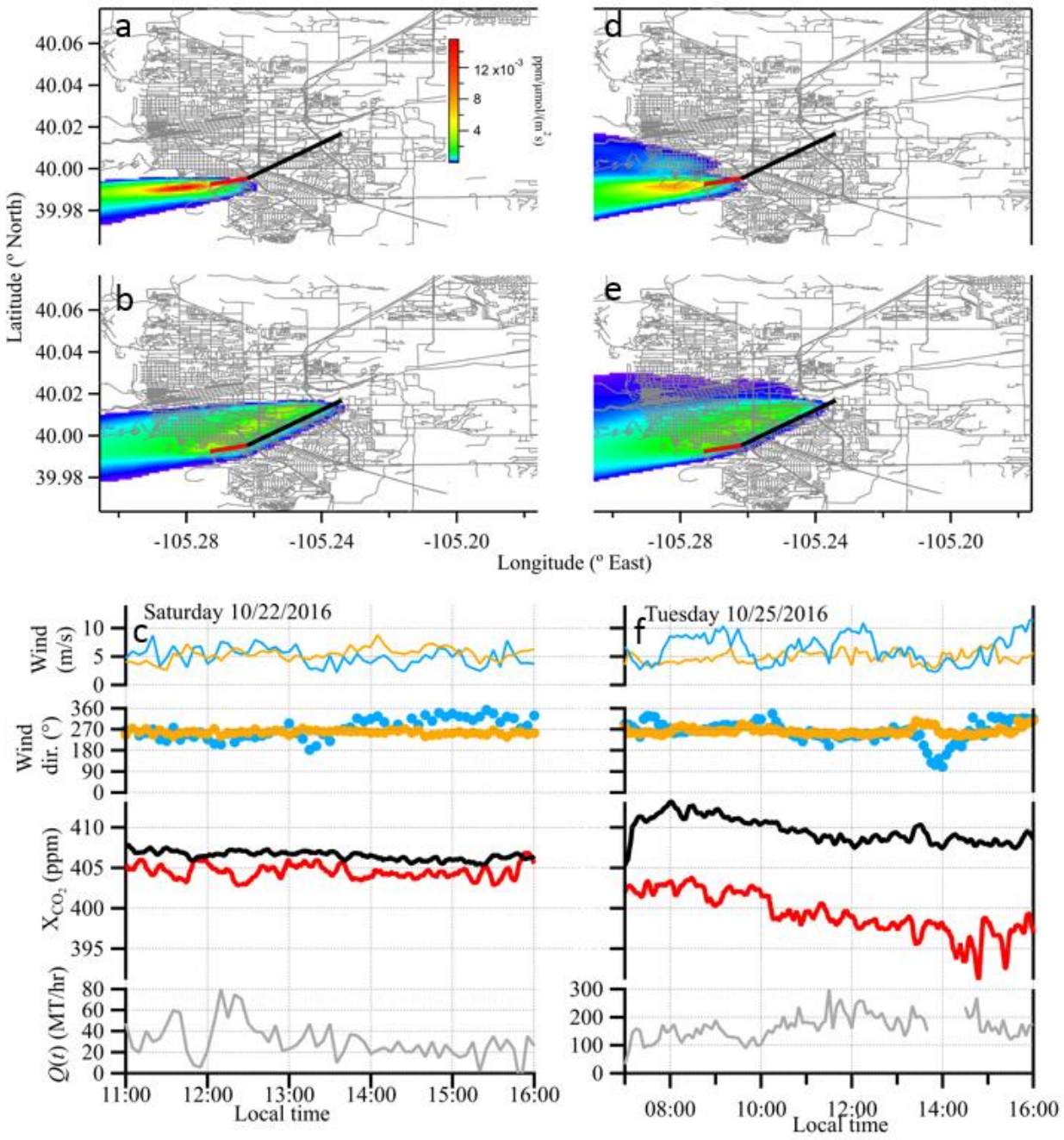

Figure 7: Footprint calculations and time series data for the two case study days. Left column: Saturday, October 22, 2016; right column: Tuesday, October 25, 2016 data. Upper panels (a, d): Footprints for the reference path. Middle panels (b, e): Footprints for the over-city path. The footprints are averaged over the respective time windows and open paths. Lower panels (c,f): Wind and CO_2 data at 5-minute time intervals. Reference and over-city measurement paths are shown in red and black, respectively. Data plots show X_{CO2} over the reference path (red) and city path (black), wind speed and wind direction measurements taken at NCAR Mesa (blue) and NCAR Foothills (orange), and the calculated $Q(t)$. On Oct. 25, $Q(t)$ data near 14:00 has been removed since the reference path wind direction is out of the southeast to east, resulting in city contamination along the reference path. All data is smoothed to 5-minute time intervals.

The modified the text at lines 289-291 read:

We attribute this variability to the smaller footprint of the reference path relative to the over-city path, as seen in Fig. 7. If the CO_2 in the air is not fully mixed, then the temporal and spatial variability will be more evident in the path with the smaller footprint.

The Q(t) time series does not indicate a peak during rush hour because all of our data indicates that Boulder only has a very weak diurnal traffic cycle. It is a sufficiently small city that the authors can anecdotally say that it does not have rush hour the same way Los Angeles or Boston or New York City has a rush hour. The Boulder rush hour is a delay of a few minutes along a drive across town. As shown in the traffic count data of Figure 4, there is only a small (~10%) bump in the traffic counts, but generally the traffic is spread out fairly evenly from 8 am to 6 pm. Similarly, there is a similar weak (~10%) peak in the Salt Lake on road emissions according to Hestia (see Mitchell et al. 2018 PNAS, Figure 2) for the DBK site which has the population density closest to Boulder (1.5e3 people/km^2, 2010 census). Thus Boulder seems to be consistent with suburbs of other urban areas. We have modified the text at lines 191-194 to read:

Note that there is only a 10-20% "peak" in traffic counts at the standard commuter times with generally high traffic levels from 7:00 to ~19:00, which agrees with the traffic emissions reported by the Hestia inventory model for the similar city of Salt Lake City, UT (Mitchell et al., 2018).

Furthermore, the description of uncertainties associated with this technique is limited. There are scattered mentioning of the uncertainties e.g., in Sect. 3.3.6. Instead, I believe a more substantial amount of text needs to be devoted to measurement uncertainties in the measurement section (Sect. 2.1). For instance, how does the uncertainty depend on path length and time resolution? Why?

We have expanded the uncertainty discussion in Section 2.1 (and moved the previous text from Section 3.3.6 to this section). We have also included a new figure showing the Allan deviation for both the city and reference paths. We note that an analysis of the systematic uncertainty (e.g. effects of the optics, detection system, and fitting parameters) was also published in Waxman et al. (2017) AMT. The new paragraph in Section 2.1 starting at line 159 reads:

The variations in the retrieved concentrations are due to statistical uncertainty, systematic uncertainty (discussed above), and the true variations in the gas concentrations. Figure 8 of (Waxman et al., 2017) quantified the statistical uncertainty in terms of the Allan deviation over the 2-km reference path for both X_{CH4} and X_{CO2}. Figure 3 here provides an Allan deviation for just X_{CO2} over both the ~6.7-km city and ~2-km reference paths, as calculated from a relatively "flat" 1000-s period of this measurement campaign on the night of 3 to 4 October 2016. As expected, the statistical uncertainty over both paths improves as the square root of integration time until reaching a floor, which we attribute to real variations in the atmospheric gas concentrations. At 30 seconds, the statistical uncertainty is 0.76 ppm for the reference path and 0.64 ppm for the over-city path, finally dropping to 0.21 ppm and 0.15 ppm, respectively, at about 15 minutes. In most subsequent figures, we show results at a 5-minute averaging time for which the statistical uncertainty is well under 0.3 ppm of X_{CO2} for both paths and therefore well below the typical atmospheric variations. Note that the uncertainty also improves with path length, as expected due to the strong absorption. The lower uncertainty over the city path reflects the expected improvement from the 3.4x longer path length lessened by the 2x reduction in return signal power also due to the longer path length.

We have also included a new Figure 3 which is the Allan deviation for both the reference and over-city paths during a three-hour time period on the night of October 3-4 which is rather flat for both paths:

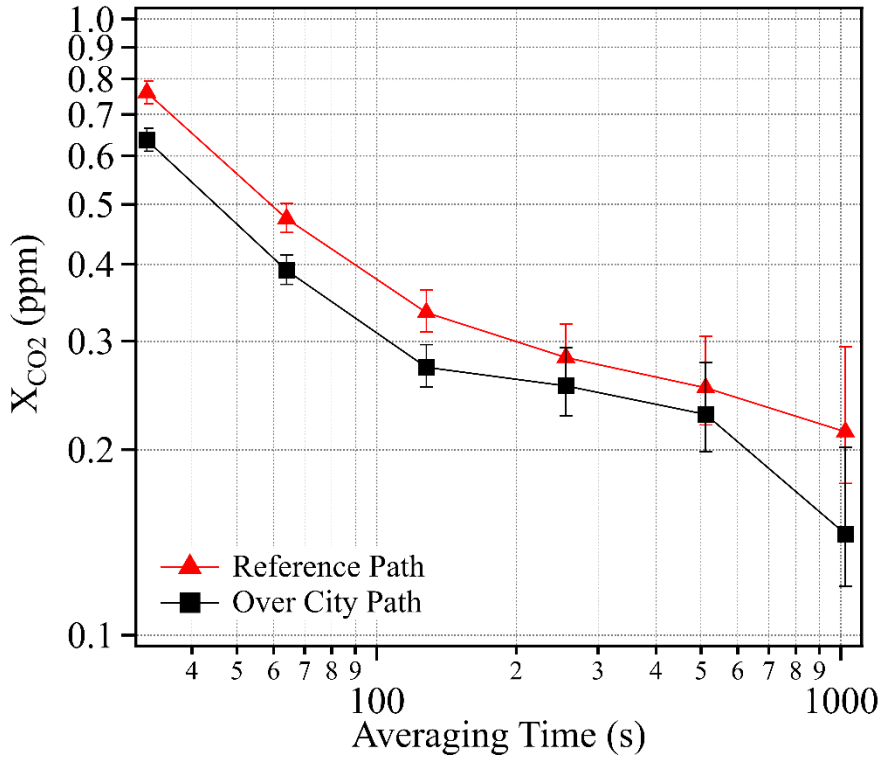

Figure 3: Statistical uncertainty as quantified by the Allan deviations for X_{CO2} over both the reference path (red triangles) and city path (black squares) from a well-mixed, three-hour time period on the night of October 3, 2016.

2) Calculation of city-wide CO2 emissions The calculation of city-wide emissions is highly unsatisfactory. The authors attribute the CO2 signal as solely due to transportation, while multiple bottom-up inventories (e.g., Vulcan, Hestia) indicate that building emissions (mainly due to heating and cooking) are non-negligible. The building emissions are neglected entirely in this paper.

*In response to this comment and the one from Reviewer 2, Comment 2 we have rewritten Section 3.3.3 to include a thorough analysis of non-traffic sources of CO_2 during our measurement time period. Unfortunately, Hestia is not yet available for Boulder and Vulcan 2.2 is only available for 2002 (14 years prior to the present study). Therefore, we cannot extract Vulcan vehicle emissions estimates for Boulder. However, we address this using the City of Boulder greenhouse gas inventory data from 2016 (*https://www-static.bouldercolorado.gov/docs/2016_Greenhouse_Gas_Emissions_Inventory_Report_FINAL-1-201803121328.pdf?_ga=2.130927943.970967930.1525795820-107394975*). This results in a correction of 14% of our calculated emission value. We have added text at lines 412-433 in Section 3.3.3 on residential emissions:*

In addition, there are also likely diffuse emissions from residential and commercial furnaces and water heaters that use natural gas. The City of Boulder Community Greenhouse Gas Emissions Inventory reports twenty percent of the city emissions, or 3.18×10^5 MT CO2e, were from natural gas in 2016 (https://www-static.bouldercolorado.gov/docs/2016_Greenhouse_Gas_Emissions_Inventory_Report_FINAL-1-201803121328.pdf?_ga=2.130927943.970967930.1525795820-107394975). The natural gas usage varies strongly by month with building heating requirements. Although our measurements occurred in October, the measurement days were quite warm (20-24 C) so that residential and commercial building heating was unlikely and the use of an annual average would overestimate any contribution. Instead, we scale the natural gas usage according to the monthly breakdown provided by the United States Energy Information Administration database for Colorado (https://www.eia.gov/dnav/ng/hist/n3010co2m.htm). The mean daytime (approximately sunrise to sunset, 7 am to 6 pm) temperature in October was 18.2 C while the mean temperature (including day and night) for October was 15.7 C. Our daytime-only measurements therefore had a mean temperature that was much closer to the mean temperature (day and night) of September, which was 19.2 C. Therefore, we scale the Boulder annual natural gas consumption by the September 2016 nature gas usage, which was 2.4% of the Colorado annual total according (https://www.eia.gov/dnav/ng/hist/n3010co2m.htm). The estimated total emissions from residential and commercial natural gas usage in Boulder over our measurement days is then 10.2 MT CO_2/hour. We apply this correction to our measured values and include a (conservative) uncertainty equal to this correction. The new adjusted values are then $Q_{Oct22,adj} = 18 \pm 20$ MT CO_2/hour for October 22 and $Q_{Oct25,adj} = 152 \pm 46$ MT CO_2/hour for October 25.

OTHER COMMENTS

What is the significance of the H2O and HDO measurements? They were shown, but no discussion is available for these species. What does HDO tell us? Are there any, say, meteorological events that can explain the variations in H2O and HDO?

The H2O measurements are required here to extract the dry mole fraction. The main significance for this work is that both paths see the same variations in these quantities, further supporting the claim that the same general air mass is sampled by the two paths so that the enhancement of carbon dioxide is attributed to local sources rather than remote sources. The variations are attributed to the normal humidity variations expected from general weather patterns but we have not conducted an analysis of these. Finally, we include HDO since it indicates the multispecies sensing capabilities of the DCS and might be useful in future analysis, but it is true that the HDO variations are not discussed at length here and the additional data plot is not strictly necessary. Discussion of the H_2O/HDO ratios and an accompanying meteorology analysis is outside the scope of this work.

We have added the following text at lines 205-207: HDO is not used here but is shown for completeness (note that the HDO concentration is scaled by the isotopic abundance in HITRAN).

And lines 214-215: The H_2O retrieval is important as accurate knowledge of the time-dependent water concentration is needed to calculate the dry CO_2 and CH_4 mole fractions (see Section 2.1).

Lines 34~36: recent high profile papers published in PNAS for the cities of Boston (Sargent et al., 2018) and Salt Lake City (Mitchell et al., 2018) should also be mentioned

We have included these references at line 43.

Lines 40~41: another key limitation for urban eddy covariance measurements is the violation of horizontal homogeneity assumptions

We thank the reviewer for the comment and have added it to the text at lines 38-39 that now reads: "…utility of this technique for large cities as do violations of the horizontal homogeneity assumption (Järvi et al., 2018)."

Lines 69~73: a reference for the CLARS instrument should be added

We have cited Wong et al. (2015) ACP, "Mapping CH4:CO_2 ratios in Los Angeles with CLARS-FTS from Mount Wilson, California" at lines 66.

Line 127: typo; should be "turbulence"

We have corrected this.

Figure 1: The satellite map of Boulder is hard to decipher. Perhaps it would be better to use a road map instead, and zoomed in more? Also need to spell out "TMC" in the caption.

We have modified the figure as suggested. In addition and in response to a similar comment by the Reviewer 2, we have changed the size of the TMC traffic symbols to indicate the traffic count. The updated figure and caption are as follows:

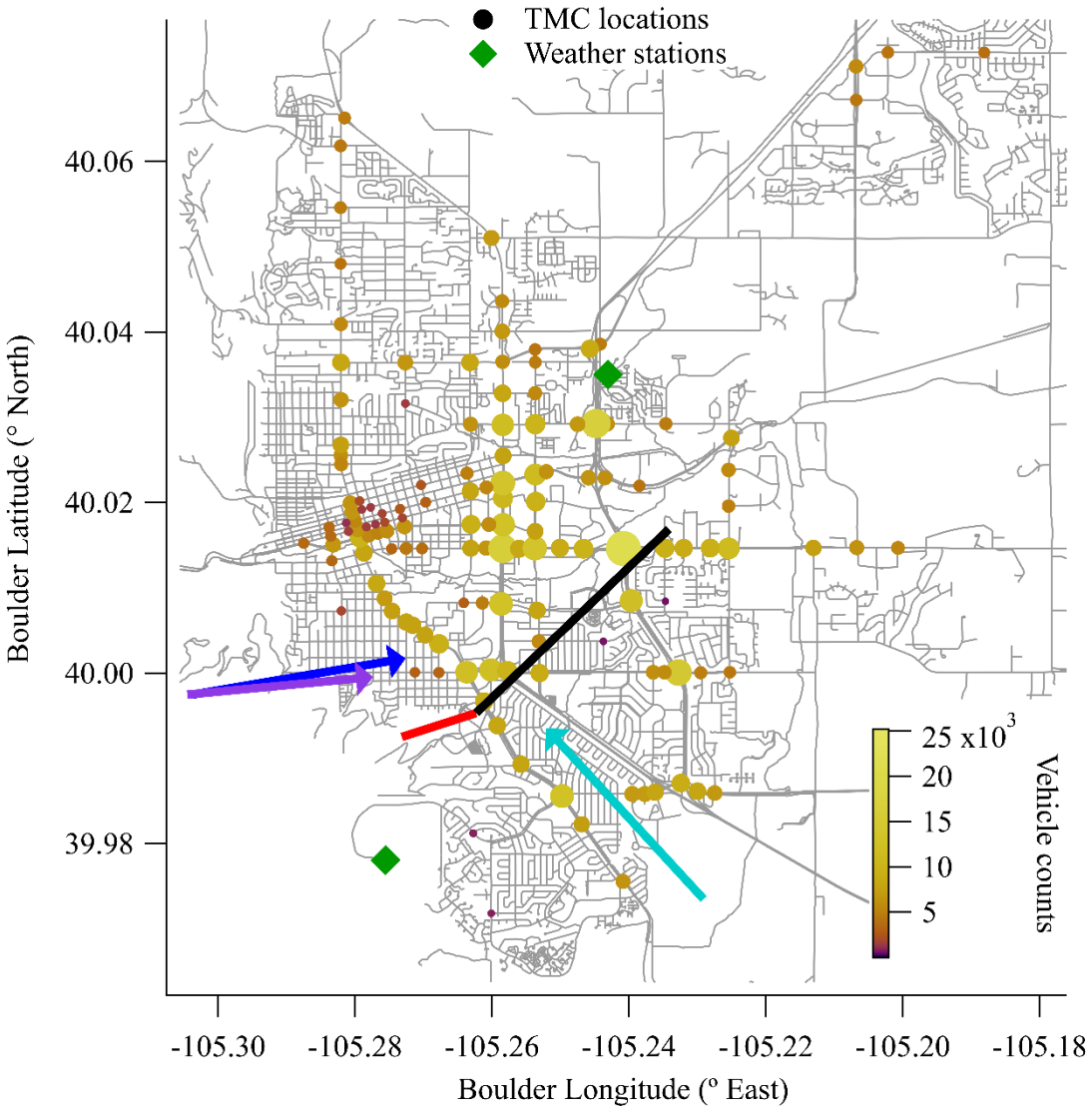

Figure 1: Measurement layout. The two measurement paths are shown by red (reference) and black (over-city) lines. The two weather stations that provided wind speed and direction data are given by the green diamonds. The colored circles are Turning Movement Count (TMC) locations, which are used as a proxy for the traffic source locations. Both color and size represent the number of traffic counts at each location. Dominant wind directions for the campaign overall (aqua) and the test case days (purple for 10/22 and blue for 10/25) are given by colored arrows.

Figure 4: Variations in all 4 species are hard to discern. Are all 7.5 weeks needed? And could the y-axis range be reduced to show more variations? And is it necessary to show all 4 species in a single panel?

We would prefer to retain all 7.5 weeks since it establishes that the DCS system is capable of this level of continuous operation, which will be needed if DCS is ever to be incorporated into long-term urban monitoring. The y-axis has been expanded almost to the peak-to-peak variations already, unfortunately. To address the reviewers valid comment, though, we have changed the aspect ratio of the figure by approximately a factor of 2. We have also smoothed the data to 5

minute integration time in order to suppress the statistical uncertainty (see Section 2.1) and enhance the true variations and differences measured across the two paths:

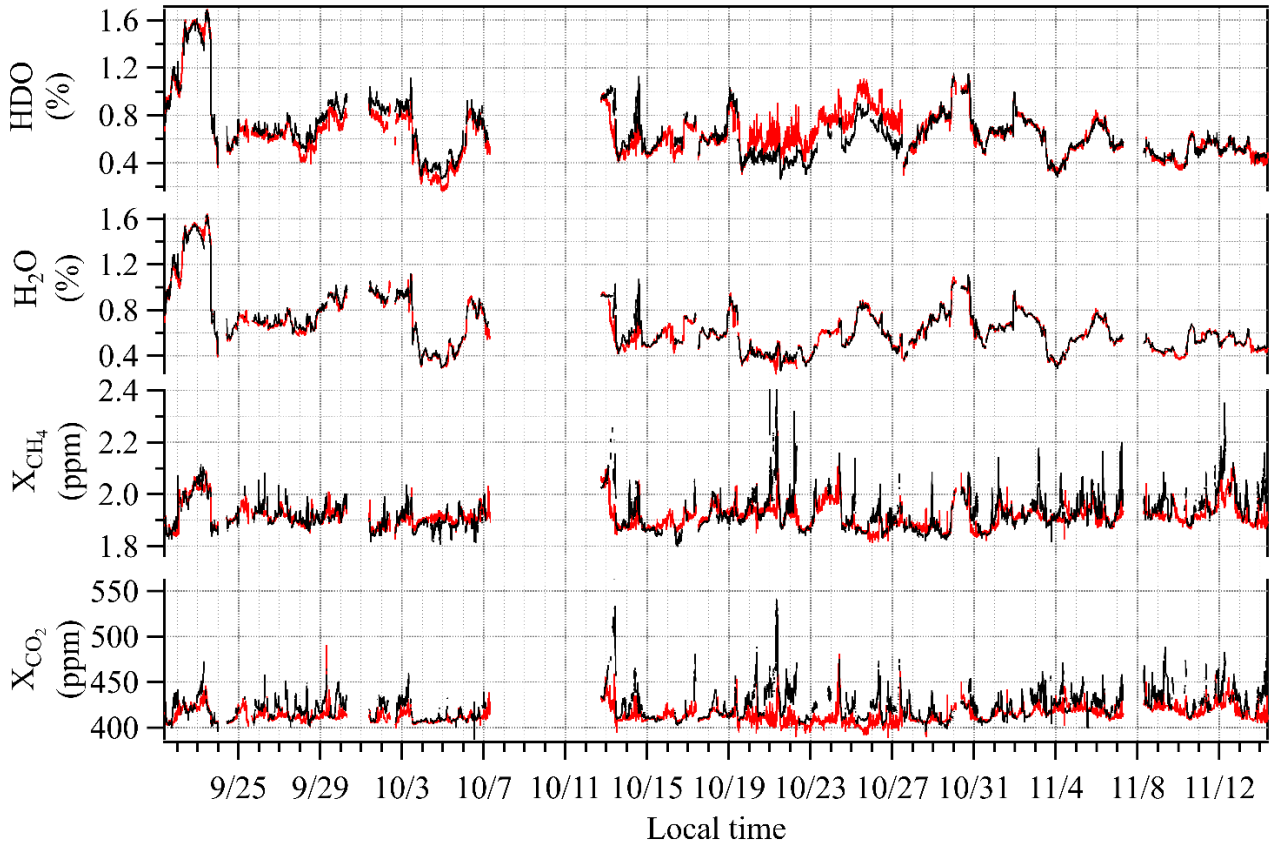

Figure 5: 7.5 weeks of dual-comb spectroscopy data for the reference path (red) and the over-city path (black) smoothed to 5-minute time intervals. Enhancements in the over-city path relative to the reference path are observed in CO_2 and CH_4 but not in H_2O or HDO. (Note: the HDO concentration includes the HITRAN isotopic scaling.)

Figure 5: There are two different copies of this figure in the PDF file. Is the first one supposed to be deleted? Here the same problem existsâA˘Tthe variations in XCO2 and ˇ XCH4 are hard to figure out. I believe the variations in the median values are the most important for the reader. Currently the differences between the blue and red symbols indicating the median values are hardly visible. The y-axis ranges can be reduced considerably to highlight variations in the medians. Are the raw data really necessary here?

As suggested by the reviewer, we have removed the raw data. However, the raw data has such a large range that we still indicate this via the uncertainty bars on the median points, which reflect the 25%-75% range of the values encountered. The y-axis has been expanded to the largest possible range that still captures this uncertainty. Following the comments of the reviewer, the revised figure is inserted below:

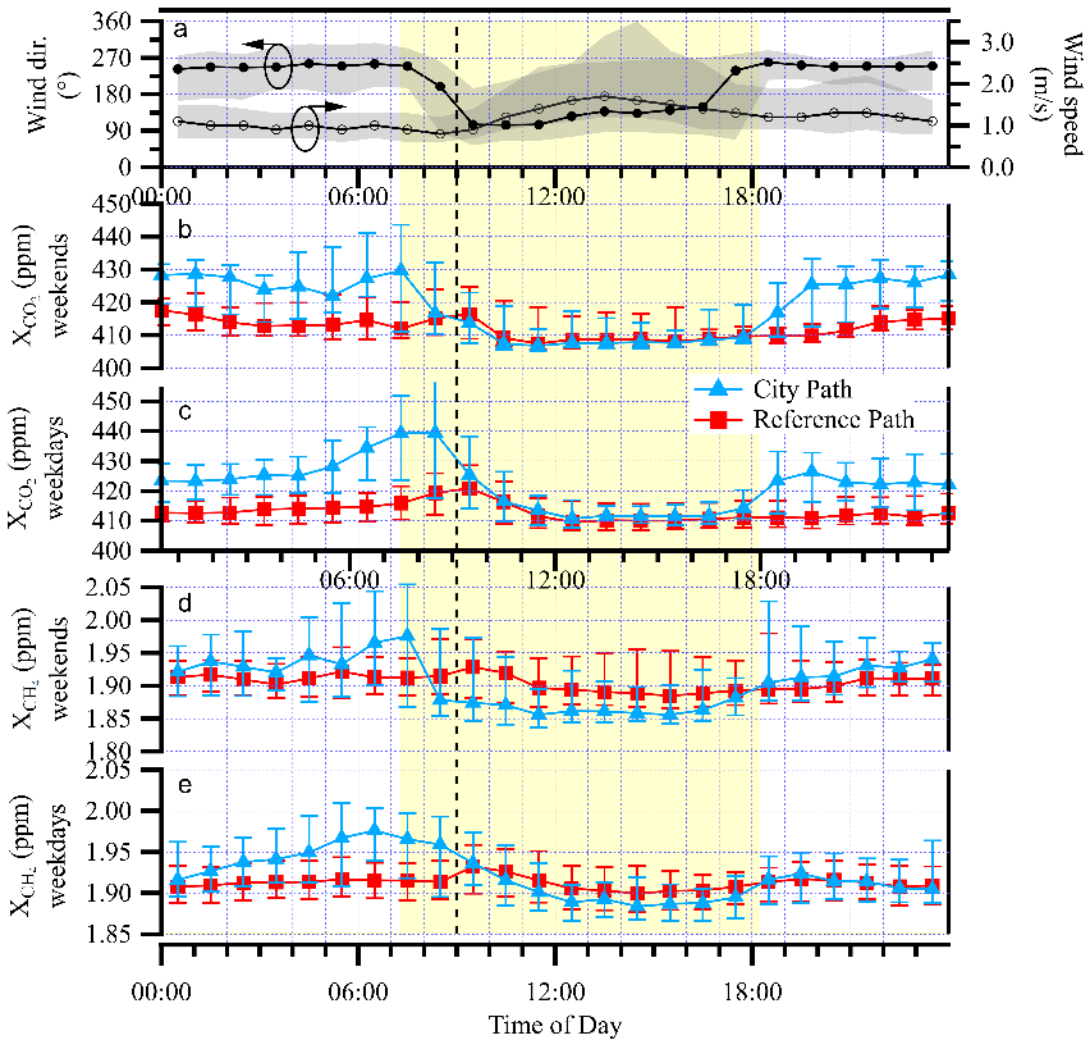

Figure 6: Diurnal cycle analysis. Data is the median of the full 7.5 weeks. (a) The mean direction in which the wind is blowing (black trace, left axis) and wind speed (gray trace, right axis) both from the NCAR Foothills measurement station, shaded regions reflect the 25th to 75th quartiles; (b) the weekend and (c) weekday median X_{CO2} values for the over-city path (blue triangles) and reference path (red squares). Uncertainty bars represent the 25%-75% range of values encountered. (d) and (e) Same data for X_{CH4}. The vertical dashed black line marks 9:00 local time and the yellow shaded region highlights the region from sunrise to sunset on Oct. 22, 2016.

Reviewer 2:

Dear the authors of the manuscript:

The study made an attempt to estimate traffic CO2 emissions from the city of Boulder using CO2 data collected from a ground-based remote sensing instrument. The team has developed and maintained their open-path dual-comb spectrometer. The instrument has been subjected to several comparisons prior to this study. The authors conducted a 7.5-week long observation (September-November) and found two time periods (10/22 (Sat) 11am-4pm and 10/25 (Tue) 10am-4pm) they think suitable for the emission estimation of this study. The authors employed a

Gaussian plume model with a city-wide traffic emission distribution constructed using the traffic data collected in Boulder, in order to estimate the annual traffic emission from the city. The estimation yielded 6.9 x 10^5 MT CO2/yr for the year 2016, which is 153% (155% in the manuscript) of the scaled city emission estimate (the 2015 traffic emission was scaled up using the total vehicle miles traveled in 2016). While several sources of errors and uncertainties due to the estimation approach were acknowledged, the authors discussed them by citing previous work, but they remained fully unquantified. The significance of this study is the application of CO2 data collected from the unique ground-based remote sensing instrument. But due to the poor design of the estimation approach and the lack of the evaluations of the results, I feel the authors failed to fully conclude this study and thus I do not recommend this manuscript for publication. I listed my major concerns and some other comments below.

1.Poor experimental design

I don't think the emission estimation was good enough to solely estimate traffic emissions. The authors had to make big assumptions to estimate annual traffic emissions from the city using two data period in 2016. Prior to the actual emission estimation, the authors needed to prove that they can get a reasonable estimation regardless of the assumptions made.

We agree with the Reviewer that we had to make large assumptions. In the revised manuscript, we have tried to be clear about those assumptions and include some estimated uncertainties. Specifically, we hope we have addressed the Reviewer's comments by 1) discussing the uncertainty of the DCS in the revised Section 2.1, 2) adding a new Section 3.3.3 that discusses the non-traffic sources and uncertainties, and 3) combining and elaborating on the scaling uncertainties in Section 3.3.4. Scaling to annual emissions is necessary as it is the only way to compare to the bottom-up inventory for the city, as we do not have an up-to-date time-resolved inventory like Vulcan or Hestia, as discussed in response to Reviewer 1 above in comment 2. Section 3.3.4 is reproduced below:

3.3.4 Scaling to annual emissions

In order to compare with the city inventory, we scale our results to an annual total. To do this, we use the hourly traffic data of Fig. 4 to scale $Q_{Oct22,adj}$ and $Q_{Oct25,adj}$ to a daily emission. Based on Figure 4, 34% of the total traffic counts occur during the 5-hour measurement period on Oct. 22 and 52% of the total traffic counts occur during the 8-hour measurement period on Oct. 25 (excluding the 13:00 to 14:00 period). The daily emissions are then $Q_{Oct22,day} = Q_{Oct22,adj} \times (5 \text{ hours}) \div (0.34)$ and $Q_{Oct25,day} = Q_{Oct25,adj} \times (8 \text{ hours}) \div (0.52)$ (The traffic data in Fig. 4 is based on weekday measurement and we assume that the hourly distribution is the same for weekends; this may lead to a slight overestimate in the weekend data where a larger fraction of emissions occurs between 11 am and 4 pm than on weekdays.) We then scale to annual emissions by assuming that the emissions on Oct. 22 are representative of all 112 weekend/holiday days and the emissions on Oct. 25 are representative of all 253 workdays. Including their uncertainty, this calculation yields $(6.2 \pm 1.8) \times 10^5$ MT CO_2/year.

The scaling relies heavily on the traffic count data supplied by the city of Boulder, which does not have an associated uncertainty value. A comparison of these data over several years shows a typical 7% statistical variation at a given TMC location, after removing a linear trend. We assume this reflects day-to-day fluctuations in traffic. In addition, there will be seasonal variations, which is not captured in the extrapolation from our two test case days to the annual emissions. Due to the lack of seasonal data for Boulder traffic, we use the detailed Hestia traffic inventory for Salt Lake City, UT given in Figure 2 of (Mitchell et al., 2018). These data show a

variation of ±18% in traffic emissions between "summer" and "winter" months. Combined in quadrature with the 7% statistical uncertainty in the TMC traffic count data, this leads to an additional ~20% uncertainty to the scaled annual estimate. As noted earlier, we have not applied any additional uncertainty on the reliance on the TMC data as a proxy for emissions locations. Including the additional uncertainty on the scaling to annual emissions, we estimate an annual emission rate of $(6.2 \pm 2.2) \times 10^5$ MT CO_2/year for traffic carbon emissions for Boulder CO.

We agree that longer time series data and different path locations would reduce the required assumptions. We discuss this in Section 4.1 in the revised manuscript:

4.1 Improvements in future measurements

Future improvements should include additional and different beam paths, selected based on prevailing wind directions. (Our initial assumption that the mountain path would generally act as a reference path was incorrect since the prevailing daytime winds are not out of the west but rather the southeast.) An east-west running beam north of the city and one south of the city would allow us to utilize a larger fraction of the data as the predominant midday wind direction during the fall is out of the north to north-east (see Fig. 1). Even longer beam paths would also interrogate a larger fraction of the city and measure a correspondingly larger fraction of the vehicle emissions. Vertically-resolved data from e.g. a series of stacked retroreflectors would better test the assumption of vertically-dispersing Gaussian plumes.

Additionally, more extensive modeling to cover variable wind directions and speeds would allow the incorporation of a much larger fraction of the data than the two days selected here. An inversion-based model similar to (Lauvaux et al., 2013) could potentially be applied to a small city like Boulder; however this would depend heavily on the quality of the bottom-up emissions inventory used to generate the priors. Indeed, one of the major future improvements would be to generate a detailed Hestia inventory of Boulder, CO similar to that generated for Salt Lake City, UT (Mitchell et al., 2018).

2. Traffic emissions

I checked the latest Boulder's inventory (2016) and their traffic emission was reduced by 10% from the previous year, which contradicts with the conclusion of this study and suggests a larger discrepancy between the authors' estimate and the inventory estimate.

We have updated the paper to compare directly to the 2016 inventory of $4.46x10^5$ MT/year (as opposed to the value used in the original submitted version of $4.52x10^5$ MT/year). As a note, the 10% reduction the reviewer cites is likely the reduction from 2005 to 2016, not 2015 to 2016. The figure from the city inventory comparison is reproduced below:

Figure 4. Emissions Comparison by Sector

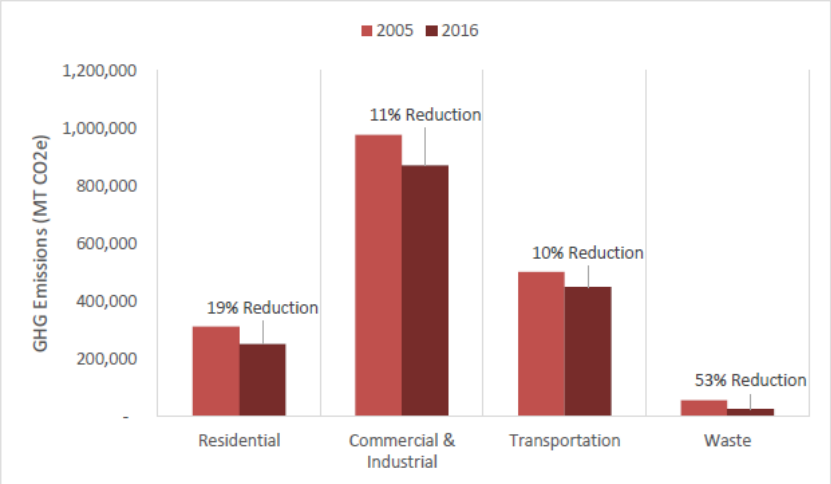

From https://www-static.bouldercolorado.gov/docs/2016_Greenhouse_Gas_Emissions_Inventory_Report_FINAL-1-201803121328.pdf?_ga=2.130927943.970967930.1525795820-1073949754.1525187370

We have edited the text at lines 470-475 to read:

The City of Boulder estimates total vehicle emissions of 4.50×10^5 metric tons (MT) of CO_2 in 2016 (https://www-static.bouldercolorado.gov/docs/2016_Greenhouse_Gas_Emissions_Inventory_Report_FINAL-1-201803121328.pdf?_ga=2.130927943.970967930.1525795820-107394975). On-road emissions account for greater than 99% of the transportation emissions, so we have scaled this value down by one percent for an on-road emissions value of 4.46×10^5 MT CO_2.

City of Boulder Community Greenhouse Gas Emission Inventory https://wwwstatic.bouldercolorado.gov/docs/2016_Greenhouse_Gas_Emissions_Inventory_Report_FINAL1-201803121328.pdf?_ga=2.75749783.365316916.1539217252-1670325792.1539217252 Given the limited observation and the simple modeling, maybe it would have been a good idea to focus on the total city emission. I do not have an access to disaggregated CO2 emissions, but traffic emissions account for 28% of the city total emission, the residential is for 16% and commercial and industrial for 54%. Ignoring the contributions from other sectors does not seem to be a good idea, especially w/o doing any source attribution analysis.

We agree with the reviewer that it would be nice to focus on the total city emissions. However, the total city emissions are calculated in such a way that we cannot do a direct comparison with our measurements, and as discussed in the updated version given the time of day, time of year, and footprints we are primarily sensitive to traffic.

The City of Boulder inventory is Scope 1 and 2 (emissions from inside the city and emissions from electricity usage when the electricity is generated outside of the city). However, our emissions measurements are Scope 1 (emissions at the location of the source). We have done

our best to account for power generation that falls within our measurement area. We discuss this is the updated 3.3.3:

There are a number of non-traffic sources of CO_2 that could contribute to our measured X_{CO2} enhancement including local power plants, residential emission, and biological activity. These non-traffic source should have relatively minor contribution for several reasons. First, the footprint of the over-city path does not overlap the large power plant to the east of the Boulder city limits. Second, the temperature during the two test case days was 24 °C and 20 °C (68 °F and 75 °F) on October 22 and 25th leading to minimal residential and commercial heating. Third, the measurements occurred in October after leaf senescence so there should be negligible biological activity. Nevertheless, as discussed below, we do adjust our measurements to account for the relatively minor contribution from non-traffic sources before scaling up to an estimate of the annual traffic emissions.

We first consider power plants. There are two power generation facilities on the Department of Commerce (DOC) campus located near the NIST building that houses the dual-comb spectrometer: the site's Central Utilities Plant (CUP), and the National Oceanic and Atmospheric Administration building's boilers. To calculate their average CO_2 emissions, we used available fuel consumption data (October 2016 monthly average for the CUP and mid-November to mid-December 2016 average for the NOAA boilers; October data was unavailable) and the EPA emissions factor (EPA, 1995). We then modeled the CUP and boiler plume emissions using WindTrax (Flesch et al., 1995, 2004) with wind speed and direction data from the NCAR-Mesa site. We find that due to the moderate wind speeds (>5 m/s) during our case study days and the height mismatch between the emission stacks and our measurement path over the DOC campus, there is negligible enhancement over the reference path. Given the location of the emission sources and the wind direction during our measurement periods, the emissions also do not cross the over-city beam path. Therefore, we apply no correction for these two power plant emissions.

The University of Colorado also has a power plant that falls within the main footprint associated with the over-city beam path, shown in Fig. 7a, and therefore whose emissions are expected to intersect our over-city beam path. The EPA Greenhouse Gas Reporting Program (GHGRP, https://www.epa.gov/ghgreporting) lists the 2017 emission from the power plant as 2.7×10^4 MT CO_2 or an average of 3.1 MT/hour. (No breakdown by season or hour is provided.) We apply this correction to our previous daily values and add an uncertainty equal to this correction in quadrature with the previous uncertainty. The new adjusted values are then 28 ± 17 MT CO_2/hour for October 22 and 162 ± 45 MT CO_2/hour for October 25.

The large Valmont power station lies just outside the city limits to the east of Boulder; however, given its location and the dominant westerly wind, emissions from this source does not reach our beam paths. There are no other power generation facilities within the city that report to the GHGRP, so we make no further corrections based on power plants.

In addition, there are also likely diffuse emissions from residential and commercial furnaces and water heaters that use natural gas. The City of Boulder Community Greenhouse Gas Emissions Inventory reports twenty percent of the city emissions, or 3.18×10^5 MT CO2e, were from natural gas in 2016 (https://www-static.bouldercolorado.gov/docs/2016_Greenhouse_Gas_Emissions_Inventory_Report_FINAL-1-201803121328.pdf?_ga=2.130927943.970967930.1525795820-107394975). The natural gas usage varies strongly by month with building heating requirements. Although our measurements occurred in October, the measurement days were quite warm (20-24 C) so that residential and

commercial building heating was unlikely and the use of an annual average would overestimate any contribution. Instead, we scale the natural gas usage according to the monthly breakdown provided by the United States Energy Information Administration database for Colorado (https://www.eia.gov/dnav/ng/hist/n3010co2m.htm). The mean daytime (approximately sunrise to sunset, 7 am to 6 pm) temperature in October was 18.2 C while the mean temperature (including day and night) for October was 15.7 C. Our daytime-only measurements therefore had a mean temperature that was much closer to the mean temperature (day and night) of September, which was 19.2 C. Therefore, we scale the Boulder annual natural gas consumption by the September 2016 nature gas usage, which was 2.4% of the Colorado annual total according (https://www.eia.gov/dnav/ng/hist/n3010co2m.htm). The estimated total emissions from residential and commercial natural gas usage in Boulder over our measurement days is then 10.2 MT CO2e/hour. We apply this correction to our measured values and include a (conservative) uncertainty equal to this correction. The new adjusted values are then $Q_{Oct22,adj}$ = 18 ± 20 MT CO_2/hour for October 22 and $Q_{Oct25,adj}$ = 152 ± 46 MT CO_2/hour for October 25.

Once leaf senescence has completed, neither plants nor soil respiration contribute to CO_2 signal (Matyssek et al., 2013). The National Phenology Network (USA National Phenology Network, 2018) data shows that for the site nearest to Boulder (64 km north of Boulder), the leaf fall dates were September 15, 2016 for box elder trees October 6, 2016 for Eastern cottonwoods. Thus by our measurement dates leaf senescence should be fully complete and plants will not contribute to the city CO_2 enhancement. We note that a wide range of biogenic contributions to CO_2 have been noted in the literature (Gurney et al., 2017; Mitchell et al., 2018; Sargent et al., 2018).

3. Background problem?

This study used CO2 data from the reference path as a background. I understand that the air must be clean for the reference data, but my concern was the authors were comparing two different airmasses to calculate the CO2 enhancement. The only supporting information of background CO2 vs. city CO2 was the wind direction from a few observation points.

We have calculated one-hour back trajectories for each hour of the case study days using STILT. These back trajectories indicate that the reference path has a much smaller footprint (as expected) but that the general airmass location is identical for the reference and city paths. Representative back trajectories and footprint calculations are now shown in Figure 7 reproduced earlier. Further, for the measurement conditions, it takes on average 18 minutes for air entering the reference path to cross the over-city path. Since the transit time is so short (i.e., it does not take multiple hours for the air to move from the reference path to the over-city path), it is unlikely that the source location of the airmass is different for the reference and over-city paths.

Please see the updated Figure 7 and related text as described in the response to Reviewer 1 above.

4. CO2-eq.

I do not understand why the authors did not use emissions in the CO2 unit, rather than in the unit of CO2-eq. In collaboration with the city council, I would imagine it is not too difficult to obtain emission estimates solely for CO2.

We have updated the units to MT CO_2/year as suggested.

5. Bottom-up vs. Top-down?

The discrepancy between bottom-up vs. top-down estimates are often large, as seen in previous studies. In many cases, the uncertainties associated with the inventory are assumed to be small. In this study, the authors have added a lot of potential errors when mapping the traffic emissions in space (approximated the spatial patterns) and time (scaled up to annual emission). Given that, less convincing than other studies if the authors did discussion just with citing papers.

As noted earlier, we have updated Section 3.3.4 to discuss the scaling more explicitly and we have included uncertainty associated with this scaling. We point out in Section 4.1 and the Conclusion that a better inventory for the city would be highly beneficial. Please see the revised Sections 3.3.4 and 4.1 above in response to Reviewer 2 Comment 1.

Other comments:

P1, L31: "top-down measurement" sounds odd to me. How about "top-down approach using atmospheric measurements"?

We have made the suggested change at line 31.

P2, L58: A SoCAB CO2 top-down study has appeared on ACPD. Check out Hedelius et al. (2018) ACPD.

We have added a reference to this work in the new text at lines 54-56: Data from the Orbiting Carbon Observatory satellite (OCO-2) was recently combined with TCCON data to estimate CO_2 emissions from the LA basin (Hedelius et al., 2018).

P4, L162-: This traffic emission modeling is based on huge assumptions. The errors and uncertainties associated with this modeling needs to be quantified at least to show if the emission estimation approach in this study has a good accuracy to show the utility of the CO2 data. Also, the authors might want to check the consistency/inconsistency between the traffic data the authors used and the new 2016 inventory used.

We have checked the consistency with the traffic data and the 2016 inventory, please see the response to "Traffic Emissions" above. We have done our best to quantify the uncertainty on our measurements and potential uncertainty due to non-traffic emissions within our measurement area as discussed above. The city does not provide any error estimates on their traffic data but we have added uncertainties as discussed above.

P6, L238: No correlations is good. . . but these are not shown anywhere.

We have updated Figure 7 and the associated text in response to a comment by Reviewer 1, please see comments above.

P8, L321: 5% sounds small, but it is comparable to the potential emission changes we want to detect. I don't think it is insignificant.

We meant that the 5% value was much smaller than our overall uncertainty. However, this statement has been removed in the revised version of the paper.

P8, L327-: I think these are another set of big assumptions. These assumptions needed to be tested. The authors cited Gurney et al. (2017), but that is a case for Indianapolis. The authors could use the same logic for the large discrepancy between the top-down and bottom-up estimates. But the authors' statements are not supported by any quantitative analyses.

As discussed above, we have expanded this paragraph to become section 3.3.3 on non-traffic sources of CO_2 (please see revised text above). To specifically respond to the discussion of biological emissions, leaf senescence is the programmed death of leaves, which occurs when the leaves change color and the chloroplasts die. After senescence has completed, plants no longer contribute to CO_2, as they are no longer photosynthesizing. Further, soil respiration is tightly coupled to photosynthesis and when photosynthesis ends, soil respiration decreases significantly. The National Phenology Network tabulates the dates of phenological events, such as leaf buds breaking, leaves turning colors, and leaves falling off trees. The site nearest to Boulder (site 20305, about 64 km north of Boulder) has a falling leaves date of September 15 for box elder trees and October 6 for Eastern cottonwoods in 2016. By late October 2016, we can expect that all of the leaves have fallen off of the trees in Boulder, and thus leaf senescence has completed. We also note that estimated plant contribution to cities varies widely with some cities (Boston, Indianapolis) finding a small but significant contribution from plants and others (Salt Lake) finding no influence from plants. Thus our results fall within the rather large reported plant influence range from the literature. We have modified he text at lines 433-439 to say:

Once leaf senescence has completed, neither plants nor soil respiration contribute to CO_2 signal (Matyssek et al., 2013). The National Phenology Network (USA National Phenology Network, 2018) data shows that for the site nearest to Boulder (64 km north of Boulder), the leaf fall dates were September 15, 2016 for box elder trees October 6, 2016 for Eastern cottonwoods. Thus by our measurement dates leaf senescence should be fully complete and plants will not contribute to the city CO_2 enhancement. We note that a wide range of biogenic contributions to CO_2 have been noted in the literature (Gurney et al., 2017; Mitchell et al., 2018; Sargent et al., 2018).

P16, Figure 1: This figure needs to be improved. It does not even clearly show the traffic distributions.

We have modified the figure as suggested by this reviewer and by the other reviewer. To address the traffic distributions, the traffic marker size now scales with traffic count. We hope the new figure is clearer.

P19, Figure 4: Given the small changes in CO2 we are discussing, I think the range of Y is too large. We can't see the variability in CO2 data.

As discussed in the response to a similar comment from the other reviewer, we have altered Figure 4 to improve the visibility of the variability.

Estimating vehicle carbon dioxide emissions from Boulder, Colorado using horizontal path-integrated column measurements

Eleanor M. Waxman[1], Kevin C. Cossel[1], Fabrizio Giorgetta[1], Gar-Wing Truong[1,2], William C. Swann[1], Ian Coddington[1], Nathan R. Newbury[1]

[1]Applied Physics Division, NIST Boulder
[2]Now at: Crystalline Mirror Solutions

Abstract

We performed seven and a half weeks of path-integrated concentration measurements of CO_2, CH_4, H_2O, and HDO over the city of Boulder, Colorado. An open-path dual-comb spectrometer simultaneously measured time-resolved data across a reference path, located near the mountains to the west of the city, and across an over-city path that intersected two-thirds of the city, including two major commuter arteries. By comparing the measured concentrations over the two paths when the wind is primarily out of the west, we observe daytime CO_2 enhancements over the city. Given the warm weather and the measurement footprint ~~of the dual-comb spectrometer over-city path~~, the dominant contribution to the CO_2 enhancement is from city vehicle traffic. We ~~We then~~ use a Gaussian plume model combined with reported city traffic patterns to estimate city emissions of on-road CO_2 as $(6.2 \pm 2.2) \times 10^5$ ~~-~~metric tons (MT) CO_2/year, after correcting for non-traffic sources. Within the uncertainty, this value agrees with the ~~compared to the~~ city bottom-up greenhouse gas inventory for the on-road vehicle sector of 4.5×10^5 MT CO_2/year. ~~The two values nearly agree to within the quoted uncertainty, which does not include additional systematic uncertainty associated in the temporal and spatial scaling of the given measurements to annual city-wide emissions.~~ Finally, we discuss experimental modifications that could lead to improved estimates from our path-integrated measurements.

1. Introduction

Measurements of greenhouse gases, especially CO_2 and CH_4, are critical for monitoring, verification, and reporting as countries and cities work towards decreasing their carbon emissions. Measurements on the city-scale are critical because cities contribute to a large fraction of global emissions (Marcotullio et al., 2013; Seto et al., 2014). However, quantification of city greenhouse gas emissions is challenging, especially for CO_2 since it has a high background and numerous point and diffuse sources including traffic, power plants, and animal and plant respiration. Emissions of pollutants are typically determined using two methods: a top-down approach using atmospheric measurements over a specific site or area to adjust a prior model, and bottom-up inventories that calculate emissions based on sector activity and sector emissions factors. Here we demonstrate a ~~new~~ technique for top-down measurements that uses an open-path sensor rather than a point sensor. ~~Significant work has been done recently to compare and reconcile these two methods for CH_4 emissions from oil and natural gas sources, e.g. (Allen, 2014; Zavala-Araiza et al., 2015) and for CO_2 in Indianapolis (Gurney et al., 2017) as well as ongoing work in Los Angeles (e.g. (Verhulst et al., 2017)), Paris (e.g. (Staufer et al., 2016)), and other cities through the Megacities Carbon Project.~~

Quantification of CO_2 fluxes from cities has ~~primarily~~ been determined from eddy covariance flux measurements with a point sensor located on a tower in or near a city~~, e.g.~~ (Nemitz et al., 2002; Velasco et al., 2005; Coutts et al., 2007; Bergeron and Strachan, 2011; Velasco et al., 2014). However, for a single sensor, the relatively small footprint of the eddy covariance flux measurements limits the utility of this technique for large cities as do violations of the horizontal homogeneity assumption (Järvi et al., 2018).

~~———~~To overcome this limitation, tower networks of point sensors can measure CO_2 at multiple sites within a city and at background sites outside the city~~, e.g.~~ (McKain et al., 2012; Lauvaux et al., 2013; Bréon et al., 2015; Staufer et al., 2016; Lauvaux et al., 2016; Shusterman et al., 2016; Mueller et al., 2017; Verhulst et al., 2017; Sargent et al., 2018; Mitchell et al., 2018). To distinguish the small

enhancements compared to the large background, these networks often use expensive, high-precision cavity ringdown (CRDS) instruments resulting in a high cost. The BEACO$_2$N network (Shusterman et al., 2016), on the other hand, has a much lower cost per sensor but requires significant calibration for quantitative results. All of these methods use an inversion to determine the total emissions and thus rely ~~heavily~~ on well-known priors and high-resolution mesoscale atmospheric models.

More recently, several other approaches ~~that do not rely as heavily on well-known priors~~ have also been applied to city-scale emissions. Aircraft mass balance measurements (White et al., 1976; Ryerson et al., 2001) have been used to determine city emissions ~~from Indianapolis~~ (Mays et al., 2009; Heimburger et al., 2017) ~~during the INFLUX campaign (Davis et al., 2017), following previous CH$_4$ emissions measurements from oil and gas fields (Karion et al., 2013, 2015). In addition, flux determination based on aircraft measurements and the divergence theorem (Conley et al., 2017) have recently been applied at the city scale.~~ However, ~~this~~ the ~~method~~ use of an aircraft is costly and labor intensive, and therefore not suited to long-term continuous measurements. Column measurements from the Total Carbon Column Observation Network (TCCON) were used to calculate total South Coast Air Basin (SoCAB) CO and CH$_4$ emissions, but not CO$_2$ (Wunch et al., 2009). ~~Satellite-based instruments have not yet quantified city CO$_2$ emissions, though OCO-2 may yield CO$_2$ emissions from megacities like Los Angeles, Riyadh, and the Pearl River Delta region (Ye et al., 2017), albeit with low temporal resolution with the current generation of satellites.~~ Data from the Orbiting Carbon Observatory satellite (OCO-2) was recently combined with TCCON data to estimate CO$_2$ emissions from the LA basin (Hedelius et al., 2018).

As an alternative to these approaches, horizontal, kilometer-scale, open-path instruments could in principle be used to determine CO$_2$ emissions from cities. Such instruments are capable of continuous measurements over a large area with a single instrument, e.g.(Wong et al., 2016; Dobler et al., 2017; Coburn et al., 2018). These sensors also have the advantage of being insensitive to small changes in local meteorology and are not subject to the same representation errors as point sensors (Ciais et al., 2010). Several such systems have been deployed. A laser absorption spectrometer system (GreenLITE) has mapped CO$_2$ concentrations over Paris, but ~~has~~ not yet ~~been used to~~ quantif~~y~~ied emissions (Dobler et al., 2017). The California Laboratory of Atmospheric Remote Sensing Fourier Transform Spectrometer (CLARS-FTS) is a downward-looking slant column Fourier transform spectrometer (FTS) that scans across 28 measurement targets in the Los Angeles Basin to measure CO$_2$, CH$_4$, and O$_2$ (Wong et al., 2015). Based on the measured CH$_4$:CO$_2$ ratio and the bottom-up CO$_2$ inventory from California Air Resources Board, researchers have calculated the LA Basin CH$_4$ emissions (Wong et al., 2016), but not yet the CO$_2$ emissions.

Here we present the quantification of city CO$_2$ emissions using open-path measurements made with a dual frequency comb spectrometer. While dual-comb spectroscopy is a relatively new technique it has a unique set of attributes that make it attractive for open path measurements (Rieker et al., 2014; Coddington et al., 2016; Waxman et al., 2017; Coburn et al., 2018). Dual-comb spectroscopy (DCS) is a high-resolution, broadband technique spanning hundreds of wavenumbers, but with a resolution that exceeds even high-end FTIRs leading to a negligible instrument lineshape. This allows for simultaneous measurements of multiple species and path-integrated temperature with low systematic uncertainty and without the need for instrument calibration. Additionally, the eye-safe, high-brightness, single transverse-mode output of a frequency comb allows for beam paths exceeding 10 km while the speed and parallelism of the measurement suppress any spectral distortion from the inevitable turbulence-induced power fluctuations over such a path. ~~The retrieved concentrations~~ Agreement in retrieved concentrations of ~~CO$_2$ and CH$_4$ between multiple~~ two DCS instruments measuring the same 1 km path~~agreed to has been shown to be as low as 0.14% for CO$_2$ and 0.35% for CH$_4$ over a 2 week period (Waxman et al., 2017).~~

Fig~~.~~ure 1 shows the measurement layout for an initial campaign to quantify CO$_2$ emissions from Boulder, Colorado. Here we take the light from a dual comb spectrometer near the edge of the city and simultaneously measure two paths: a reference path that points west-southwest towards the mountains and an over-city path that crosses the city to the northeast, covering the main traffic arteries of the city with sensitivity to traffic emissions. ~~-~~We acquire time-resolved data at 5~~32-~~minute~~second~~ resolution of CO$_2$,

CH_4, H_2O and isotopologues over 7.5 weeks. The dry mole fraction of CO_2 ~~and CH_4~~ shows a diurnal cycle ~~expected from~~consistent with anthropogenic sources. In addition, there is a distinct difference between the weekday and weekend cycles for CO_2, consistent with traffic patterns. In order to demonstrate the utility of this method for emissions quantification, we perform a preliminary estimate of the CO_2 emissions from traffic. To ~~estimate the total carbon emission from traffic~~do this, we filter the data for days when the wind is out of the west and not too strong so that there is a measurable daytime enhancement in CO_2 between the reference path and over-city path. Given the weather, beam path location, and observation times, ~~and based on related inventory models,~~ the dominant contribution will be from traffic rather than residential or industrial emissions. We ~~then~~ apply a Gaussian plume model to calculate the city emissions based on the expected distributed source (due to traffic) and the path-averaged concentrations. ~~Given the weather, beam path location, and observation times, and based on related inventory models, the dominant contribution will be from traffic rather than residential or industrial emissions.~~ ~~second estimate of the city emissions based on the same traffic inventory and path-averaged concentrations~~ After adjusting for small expected contributions from residential sources and a local utility plant ~~based on inventory model~~, the measured ~~This~~ emission value is scaled to annual city-wide emissions based on city traffic count data. We estimate $(6.2 \pm 2.2) \times 10^5$ metric tons (MT) CO_2/year, ~~metric tons (MT) CO_2/year,~~ compared to the bottom-up City of Boulder inventory estimate of 4.46×10^5 MT CO_2/year. Finally, we discuss improvements to this estimate, which could be realized by more advantageous beam paths that sample a larger spatial and temporal fraction of the full city emissions and by a more detailed inventory model.

2. Experimental data

2.1 DCS measurements

The dual frequency comb spectroscopy (DCS) system was located on the top floor of the National Institute of Standards and Technology (NIST) building in Boulder, Colorado. This instrument has been described previously (Truong et al., 2016; Waxman et al., 2017). The light from the combs is split to generate two combined dual-comb outputs, one of which is transmitted over the reference path and one of which is transmitted over the city path (see Fig. 1.) Here, we transmit 2-10 mW of light spanning 1.561 to 1.656 μm, which includes absorption lines from CO_2, CH_4, H_2O and HDO. The returning light from each path is detected and digitized to yield the transmitted optical spectrum at a point spacing of 0.0067 cm^{-1} (1.5 picometer) and with effectively perfect (10 ppb) frequency accuracy and narrow instrument lineshape (~4×10^{-6} cm^{-1}). A typical spectrum from the reference path is shown in Fig. 2. A fit of this transmitted spectrum yields the path-averaged gas concentrations. The absolute frequency accuracy and high frequency resolution of the dual-comb spectrometers translates to a high precision and accuracy in the retrieved concentrations. Further, DCS spectra are undistorted by turbulence due to the simultaneous acquisition of all spectral channels and the fast sample rate of the instrument (1.6 ms/spectrum, averaged up to 5 minutes here~~32 seconds~~) (Rieker et al., 2014).

In previous work (Waxman et al., 2017), we confirmed the high precision and accuracy possible with open-path DCS. ~~Previously,~~ T~~t~~wo DCS instruments, constructed by different teams, measured~~ing~~ atmospheric air over adjacent paths ~~were compared~~ over a two-week period. The ~~and~~ retrieved path-averaged gas concentrations ~~were found to~~ agreed to better than 0.6 ppm (0.14%) for CO_2 and 7 ppb (0.35%) for CH_4 across the full two week period, where the analysis of the two DCS instruments used a common spectral database (HITRAN 2008, Rothman et al., 2009) to retrieve the concentrations from the absorption spectrum. ~~(Waxman et al., 2017).~~ ~~(~~In the work here, a single DCS instrument probes the concentrations across two different open paths simultaneously, which should further suppress any systematic offsets to below 0.45~~6~~ ppm~~.~~ (Waxman et al., 2017).~~)~~ ~~Further, DCS spectra are undistorted by turbulence due to the simultaneous acquisition of all spectral channels and the fast sample rate of the instrument (1.6 ms/spectrum, averaged up to 32 seconds) (Rieker et al., 2014).~~ In addition, ~~in~~ (Waxman et al., 2017) ~~we~~ compared ~~to the comparison between~~ the two DCS instruments~~s, we performed a~~

~~comparison with~~ to a stationary cavity ringdown (CRDS) point sensor whose inlet was approximately at the midpoint of ~~ in (Waxman et al., 2017) that was located along our reference p~~the open path. This comparison actually took place over the reference path ~~occurred~~ during the first two weeks of the present work. During that time, we found a roughly constant difference of 3.4 ppm CO_2 and 17 ppb CH_4 between the DCS and CRDS systems. At present, we attribute this~~e~~ offset to differences in the calibration scheme as the DCS ~~uses~~is tied to the HITRAN ~~directly~~database ~~(see below)~~ while the CRDS is tied to the manometric (~~and~~or gravimetric depending on the gas) WMO scale. Similar level offsets have been observed in comparison of the TCCON open-path FTS instrument and point sensor-based vertical columns~~s~~ ~~(xxxx)~~resulting in the TCCON CO_2 scaling factor of 0.9898 (4.08 ppm for a mixing ratio of 400 ppm) (Wunch et al., 2015). This offset does not affect the results here as it is common to both the reference and over-city paths.

The reference and over-city paths had different path lengths and therefore used slightly different telescopes and launch powers. For the reference path, 2 mW of dual-comb light is launched from a 2-inch home-built off-axis telescope (Cossel et al., 2017; Waxman et al., 2017). The light travels to a 2.5-inch retroreflector located on a hilltop 1 km to the southwest of NIST and then is reflected back to a detector that is co-located with the launch telescope for a 1950.17 ± 0.15 m round-trip path. Return powers vary constantly with air turbul~~e~~ance but we collect about 200 μW for a typical 10 dB link loss. For the city path, 10 mW of dual-comb light is launched from a modified 10-inch diameter astronomical telescope to a 5-inch retroreflector located on a building roof 3.35 km to the northeast for a 6730.66 ± 0.15 m round-trip path. We collect about 100 μW for a typical 20 dB link loss. Round-trip path distances were measured with a laser range finder. Telescope tracking of the retroreflector is implemented to compensate for thermal drifts via a co-aligned 850 nm light emitting diode (LED) and Silicon CCD camera (Cossel et al., 2017; Waxman et al., 2017).

The measured spectra are analyzed as described in (Rieker et al., 2014; Waxman et al., 2017) at 32 second intervals. Briefly, we fit a 7th-order polynomial and HITRAN data to the measured spectrum in 100-GHz (0.333 cm^{-1}) sections to remove the underlying structure from the comb themselves (as opposed to the atmospheric absorption). We fit the resulting absorption spectrum twice: once in the region from 6171 cm^{-1} to 6271 cm^{-1} ~~185-188 THz~~ (1.595 to 1.620 μm) to obtain the path-averaged temperature from the 1.6 μm CO_2 band, and once over the entire spectrum to obtain $^{12}CO_2$, $^{13}CO_2$, CH_4, H_2O, and HDO concentrations using the retrieved temperature. We then use the retrieved H_2O concentration to correct the wet CO_2 and CH_4 mole fractions to dry mole fractions, hereafter referred to as X_{CO2} and X_{CH4} given in units of ppm and ppb (micromole of CO_2 per mole of dry air, and nanomole of CH_4 per mole of dry air). The correction equations are $X_{CO2} = CO_2/(1-H_2O)$ and $X_{CH4} = CH_4/(1-H_2O)$.

The variations in the retrieved concentrations are due to statistical uncertainty, ~~variations in the~~ systematic uncertainty (discussed above), and the true variations in the gas concentrations. ~~For the systematic uncertainties For a complete analysis of DCS uncertainty, please see Table 2 of (Waxman et al., 2017) and the related discussion, which . Based on this reference, we would expectgive a maximum systematic uncertainty of 0.6 ppm X_{CO2} between two DCS systems. Here the systematic uncertainty is here and likely muchy lower due to the use of a single DCS instrument. .~~ Figure 8 of (Waxman et al., 2017) ~~previously~~ quantified~~gave~~ the statistical uncertainty~~,~~ in terms of the Allan deviation~~,~~ over the 2-km reference path for both X_{CH4} and X_{CO2}. Figure 3~~2X~~ here provides an Allan deviation for just X_{CO2} over both the ~6.7-km city and ~2-km reference paths, as calculated from a relatively "flat" 1000-s period of this measurement campaign on the night of 3 to 4 October 2016. As expected, the statistical uncertainty over both paths improves as the square root of integration time until reaching a floor, which we attribute to real variations in the atmospheric gas concentrations. At 30 seconds, the statistical uncertainty of $X_{CO2}$is 0.76 ppm for the reference path and 0.64 ppm for the over-city path, finally dropping to 0.21 ppm and 0.15 ppm, respectively, at about 15 minutes. In most subsequent figures, we show results at a 5-minute averaging time for which the statistical uncertainty is well under 0.3 ppm of X_{CO2} for both paths and therefore well ~~, or~~ below the typical atmospheric variations. Note that the uncertainty also improves with path length, as expected due to the stronger absorption.~~In terms of instrument uncertainty, the~~

~~precision of the retrieved CO_2 is 0.769 ppm for the reference path at our 30-second time resolution (Waxman et al., 2017) and 0.564 ppm for the over-city path.~~ The lower uncertainty over the city path reflects the expected improvement from the 3.4x longer path length lessened by the ~~The precision is better over the longer path because the absorption lines are stronger which improves our signal to noise, but the precision does not improve linearly with path length because~~ 2x reduction in return signal power for the longer path length ~~we have substantially lower light return over the 6.7 km path (see Section 2.1) which worsens our signal to noise~~. ~~at least 1000 s, 0.210.1515. Our Allan deviation is limited to approximately 1000 seconds because of variations in the atmospheric gas concentration, especially across the city path, which limits the extent of the relatively flat measurement time period.that is attributed to true variations in the atmospheric gas concentrations. .~~

2.2 Meteorological Measurements

Meteorological data including pressure, wind direction, and wind speed measurements are obtained from meteorological stations located at NCAR-Mesa and NCAR-Foothills (~~ftp://ftp.eol.ucar.edu/pub/archive/weather~~ftp://ftp.eol.ucar.edu/pub/archive/weather), which are approximately the endpoints of our measurement paths (see Fig. 1), as well as a 3-D sonic anemometer located at NIST. The path-averaged air temperature was retrieved from the CO_2 spectra as described above.

2.3 Traffic data

We measure a subset of Boulder traffic, so we use the city traffic data to determine the fraction covered by our footprint (see Fig. 1). Traffic data from the City of Boulder is freely available at: https://maps.bouldercolorado.gov/traffic-counts/?_ga=2.264109964.1414067815.1500302174-274759643.1492121882. The city provides two types of traffic data that are useful in this work: ~~-~~the Arterial Count Program (ART) and the Turning Movement Count (TMC) data.

ART measures traffic at 18 major intersections in Boulder for five days (one work week, Monday through Friday) every year in one-hour bins to create a diurnal cycle. The traffic counts for 2016 are shown in Fig. 4~~3~~. We use these data to scale our selected measurement time periods to a full day as discussed in section 3.3.4. Note that there is only a 10-20% "peak" in traffic counts at the standard commuter times ~~and, to lowest order, the~~with generally high traffic levels ~~is consistently high~~ from 7:00 to ~19:00, which ~~is~~ agrees with the traffic emissions reported by the Hestia inventory model for the similar city of Salt Lake City, UT (Mitchell et al., 2018).

TMC measures the number of vehicles at 140 intersections in Boulder for one work day per year during the hours of 7:45-8:45, 12:00-13:00, and 16:45-17:45. One third of each of these sites is measured every year. We have scaled the 2014 and 2015 data to 2016 traffic levels by using total vehicle mile values available from the City of Boulder. We approximate ~~the location of~~ city vehicle emissions by using the TMC locations as our ~~Gaussian plume~~ source locations with ~~the~~ a source strength~~s~~ scaled based on the location's fractional traffic count. ~~(See Section 3.3.2).~~

3 Results and Discussion

3.1 DCS measurements

All 7.5 weeks of DCS measurements of CO_2, CH_4, H_2O, and HDO are shown in Fig. 5~~4~~. HDO is not used here but is shown for completeness (note that the HDO concentration is scaled by the isotopic abundance in HITRAN). We have insufficient precision to measure time-resolved $^{13}CO_2$ concentrations over the 2-km path. However, there are very clear enhancements in the over-city path relative to the reference path for the other trace gases, especially for CO_2. These enhancements are observed primarily at night when the boundary layer is lower. For example, on Oct. 13 the CO_2 enhancement reaches 129 ppm and the CH_4 enhancement reaches 265 ppb. Daytime enhancements occur when the wind speed is very low and intermittent (typically below 5 m/s), which allows emitted gases to build up over the city.

When the wind increases to steady moderate speeds, the concentrations drop quickly as the emissions are flushed out of the city. The H_2O retrieval is important as ~~is shown as it is necessary to~~ accurate knowledge of the time-dependent water concentration is needed ~~in order~~ to calculate the dry CO_2 and CH_4 mole fractions (see Section 2.1). Also, ~~T~~the correlation of the water concentration between the two paths ~~also~~ indicates the two paths~~y~~ sense the same air mass, which is further substantiated in Figure 7a and is ~~important~~central to ~~in~~ attributing their different CO2 concentration to local urban sources.
~~and~~

3.2 Diurnal Cycles

The diurnal cycle of X_{CO2} and X_{CH4} for both the reference path and the over city path are shown in Fig. 6~~5~~ for weekdays (midnight to midnight Monday through Friday) and weekends (midnight to midnight Saturday and Sunday). We choose to include Monday as a weekday and Saturday as a weekend because the influence of emissions from the previous day is expected to be low. The diurnal cycle of the wind direction and the wind speed measured at NCAR Foothills are also shown in the top panel of Fig. 6~~5~~. All diurnal cycles are the median values over the full 7.5 weeks of measurements and the bars ~~encompass~~reflect the 25%/75% quartile valuess.

The diurnal cycle of the reference path CO_2 is nearly flat and nearly identical for both weekends and weekdays. It has ~~only~~ a slight maximum between 9 and 10 am, with average values of 410 to 420 ppm. ~~The flatness of these diurnal cycles supports our assumption that this path represents the reference air entering the city, as there is no buildup over the course of the night as the boundary layer drops.~~ The diurnal cycle of the city path CO_2 shows a different trend with a stronger diurnal variation. Overnight from about 6 pm (18:00) to 9 am, there is an enhancement in the CO_2 relative to the reference path as the CO_2 from the city sources builds up due to the low winds out of the west and a presumed collapsing nighttime boundary layer. During the weekdays, this enhancement increases in the morning consistent with the rise in ~~a commuter~~ traffic ~~peak~~. After the morning, the combination of the presumed rising boundary layer, increased wind speed, and shift in average wind direction out of the west (270°) to the southeast (135 °) result in a drop in the city path CO_2~~.~~. Moreover, this shift in wind direction means that the ~~so that it matches the nominal~~ reference path no longer samples the clean air from the direction of the mountains but rather sees a ~~-~~very similar CO_2 enhancement as the city path. ~~.~~ (Fortunately, as discussed below, there are days when the wind does not shift direction so that there is a measured enhancement of the city path compared to the reference path.) In the early evening, as the wind speed drops and the wind direction shifts back to out of the west, the ~~buildup~~ enhancement of the city path over the reference path reappears and continues overnight as the boundary layer presumably drops. In general, the CO_2 mixing ratios tend to be higher on the weekdays, sometimes exceeding 500 ppm, while weekend mixing ratios are entirely below 490 ppm. This difference is reflected in the median values as well, which reach about 440 ppm during the weekdays but only 430 ppm during the weekend.

The diurnal cycle of the reference path CH_4 is relatively flat for both weekends and weekdays at just over 1.9 ppm, with a slight peak between 9 and 10 am. The diurnal cycle of the city path CH_4 shows an enhancement, relative to the reference path, between midnight and about 9 am. We attribute this enhancement to sources of CH_4 within the city combined again with low nighttime winds and collapsing boundary layer. These sources may be leaking natural gas infrastructure such as observed in Boston (Phillips et al., 2013; McKain et al., 2015; Hendrick et al., 2016), Washington, D.C. (Jackson et al., 2014), and Indianapolis (Lamb et al., 2016). Unlike for CO_2, the CH_4 diurnal cycle appears unrelated to traffic (nor would we expect it to be for clean-burning vehicles) as it does not increase during ~~peak~~ high traffic times.

3.3 Estimate for CO_2 emissions due to traffic

3.3.1 Measurement day selections

To select test case days to estimate the city emissions, we filter the X_{CO2} time series for time periods with daytime enhancement and a moderate wind strength predominantly out of the west (270 °). Given that the prevailing daytime winds are from the southeast (135°) and often strong, this limits the test

case days significantly. However, as is clear from Fig. 1, for these wind conditions, the city path samples a significant fraction of the traffic emissions and the reference path samples no traffic emissions. We consider only daytime enhancements because the nighttime boundary layer behavior is significantly more complicated than a well-mixed daytime stable boundary layer. We find two days that meet these criteria: Saturday 22 October 2016 from 11:00 to 16:00. and Tuesday 25 October 2016 from ~~10~~7:00 to 16:00. Both days have moderate wind speeds (on average, 5 m/s) as measured at both meteorological sites. There are additional days with daytime enhancement in X_{CO2}, but the wind direction is variable. Additionally, there are many days with no daytime enhancement in X_{CO2} because the high wind speeds (6 m/s or higher) prevented buildup of CO_2. We use Oct. 22 as a proxy for all weekend days and Oct. 25 as a proxy for all weekdays. The X_{CO2} and X_{CH4} mixing ratios as well as wind speed and wind direction for these two case study days are shown in Fig. ~~6~~7.

In order to confirm that the reference path measured clean background air and the over-city path~~s~~ measured city emissions ~~were sampling the desired sources~~, we calculated footprints for the two test case time periods using the Stochastic Time-Inverted Lagrangian Transport (STILT-R) model (Fasoli et al., 2018). ~~Average footprints for the two time periods are shown in Fig 7. We used a simple~~The input meteorology file consist~~ing~~ed of a uniform wind field with wind data from the NCAR Foothills lab, boundary layer height from the North American Regional Reanalysis (NARR), ~~and~~ uniform turbulent velocity variance calculated from the Pasquill stability class (determined from wind speed and solar insolation) from the ground up to the boundary layer, and ~~. We used~~ the hyper near-field scaling described in Fasoli et al., (2018)~~What goes here?(Fasoli et al., 2018)Fasoli 2018~~. Average footprints for the two time periods are shown in Fig 7. The footprint for the reference path covers undeveloped areas ~~without traffic~~ extending from the near foothills into the mountains. The footprint for the over-city path also has contributions from the same general mountain region. In addition, this path~~it~~ has sensitivity to ~~the~~an extended area within the city ~~that overlaps a large fraction of the traffic, as discussed below~~and therefore to a large fraction of the traffic emissions. Note the open-path geometry leads to a much larger extended footprint for this path than would be the case for a single point sensor located at the same height within the city.

The variability in the reference CO_2 on both days is a real atmospheric effect. (In processing, any data is removed if the signal power is low, which is indicative of poor telescope alignment or strong weather-related attenuation over the beam path, so the variability is not due to variable signal strength.)~~.~~ ~~We observe a weak correlation of the variability with the NCAR Mesa wind speed – approximately 5 minutes prior to most drops in CO_2 there is a spike in the wind speed suggesting that a gust of very clean air has crossed the measurement path. We see no correlations with other meteorological variables (e.g. temperature, wind direction, pressure).~~We attribute this variability to the smaller footprint of the reference path relative to the over-city path, as seen in Fig. 7~~a, c panels a, b, d, and c~~. If the CO_2 in the air is not fully mixed, then the temporal and spatial variability will be more evident in the path with the smaller footprint.

To convert from the measured enhancement to an emissions rate, we require a model that connects the source strength to the plume concentration. ~~Here~~Since we do not have a high-resolution, spatially resolved inventory for Boulder~~, as described below,~~ similar to the Hestia model for Salt Lake City (Mitchell et al., 2018)~~ (XXX)~~, we use the existing Boulder traffic inventory (see Section 2.3) in conjunction with ~~for this initial demonstration we use~~ a Gaussian plume model.

3.3.2 Gaussian plume calculations

The standard Gaussian plume model that includes total reflection at the Earth's surface is (Seinfeld and Pandis, 2006):

$$c(x,y,z,t) = \frac{q}{2\pi\sigma_y\sigma_z u}\exp\left(\frac{-(y-y_0)^2}{2\sigma_y^2}\right)\left[\exp\left(\frac{-(z-H)^2}{2\sigma_z^2}\right)+\exp\left(\frac{-(z+H)^2}{2\sigma_z^2}\right)\right] \quad (1)$$

where (x,y,z) is the location in space for which the plume concentration is being calculated, (x_0,y_0,H) is the emissions location, $c(x,y,z)$ is the concentration at location (x,y,z) and time t, q is the emissions strength (usually in kg/s), σ_y and σ_z are the plume variances in the y and z direction as a function of travel distance and Pasquill stability class (Seinfeld and Pandis, 2006), and ~~-~~u is the wind speed in m/s. The wind is assumed to be in the x-direction. The plume variances are calculated as:

$$\sigma_y = \exp\left[I_y + J_y(\ln \Delta x) + K_y(\ln \Delta x)^2 \right] \quad (2)$$

and

$$\sigma_z = \exp\left[I_z + J_z(\ln \Delta x) + K_z(\ln \Delta x)^2 \right] \quad (3)$$

where I_y, J_y, K_y, I_z, J_z, and K_z are from a look-up table based on the Pasquill stability class, which depends on the wind speed and solar insolation (Seinfeld and Pandis, 2006) and Δx is the x-distance relative to the plume origin. This plume model does not include any reflection at the boundary layer height; however, due to the small spatial scales, this effect is negligible here.

We modify this equation in several ways: 1) ~~-~~Since we measure the column-integrated concentration over a finite beam path at an angle to the wind direction, we integrate the plume concentration along this beam path and then normalize to the length of the beam path. 2) We sum over the emissions locations in the city that contribute emissions to our measurements. Thus our overall measurement equation is:

$$(c - c_0) = \frac{Q}{L} \sum_{(x_j,y_j)} \int_0^L \frac{f_j}{2\pi\sigma_y\sigma_z u} \exp\left(\frac{-(s\sin\theta - y_j)^2}{2\sigma_y^2} \right) \left[\exp\left(\frac{-(15-1)^2}{2\sigma_z^2} \right) + \exp\left(\frac{-(15+1)^2}{2\sigma_z^2} \right) \right] ds \quad (4)$$

where $(c - c_0)$ is our path-integrated concentration enhancement measurement ~~along our path s~~ (in MT/m^3 and MT is metric tons; 1 MT = 1000 kg)~~,~~ along our path s which goes from 0 to L, Q is the total city emissions in MT/~~year~~day~~hour~~, L ~~-~~is our path length in m, (x_j, y_j) are the source emissions locations, f_j ~~-~~is the fraction of traffic at source location (x_j,y_j) relative to traffic over all locations in the city from the TMC database, u ~~-~~is the wind speed in m/s, θ ~~-~~is the angle of the beam path with respect to the wind direction, and σ_y and σ_z are the plume dispersions in m in the y and z directions, which depend on the sources distance from the beam path. In writing (4), we assume the wind is in the $+\hat{x}$ direction (which assumption is relaxed below). We assume that all plume emission~~s~~ locations are ~~emitted from~~ vehicle tailpipes at 1 m above the ground, and the beam path runs 15 m above ground so all measurement heights are at 15 m above ground.

Grid rotation for variable wind directions

To calculate (4), we grid the emissions locations using UTM (Universal Transverse Mercator) coordinates obtained from Google Earth, where we then define north as $+\hat{y}$ and east as $+\hat{x}$. We translate the coordinate system such that the DCS path begins at the origin (0,0) and travels a distance L at angle θ ~~-~~with respect to the x-axis. Eq. (4) is then valid provided the wind is directly in the $+\hat{x}$ direction. More generally, the wind is at a time varying small angle $\phi(t)$ with respect to $+\hat{x}$. Therefore, we apply a rotation about the origin (Prussin et al., 2015):

$$\begin{bmatrix} \cos\phi & \sin\phi \\ -\sin\phi & \cos\phi \end{bmatrix} \begin{bmatrix} x \\ y \end{bmatrix} = \begin{bmatrix} x' \\ y' \end{bmatrix}$$

to generate new traffic coordinates (x_j', y_j') and a new parameterized DCS beam path of $(s\cos(\theta'), s\sin(\theta'))$ where ~~s goes from 0 to~~ L ~~and~~ $\theta' = \theta - \phi(t)$. In this new coordinate system, the wind is along the $+\hat{x}$ direction and Eq. (4) holds with the substitutions $\theta \rightarrow \theta'$ and $y_j \rightarrow y_j'$, and where the σ_y and σ_z are calculated based on the distance ~~δ~~$\Delta x = |x_j' - (s_j \cos\theta' y_j'/\tan\theta')|$ ~~where $s_j \sin\theta' = y_j$~~.

Time dependent estimate of $Q(t)$

The rotated Eq. *(4)* can be solved for Q in terms of the measured or estimated values of $c(t)$-$c_0(t)$, $u(t)$, $\Delta\phi(t)$, $\sigma_y(t)$, $\sigma_z(t)$, θ, L, and f_i, where the first five quantities are time dependent. The resulting, time-dependent $Q(t)$ for each test case day is shown in the bottom panels of Fig. 7~~6~~ and has a mean value and standard deviation of $Q_{Oct22} = 31 \pm 17$ MT CO_2/~~year~~ hour for October 22 and $Q_{Oct25} = 165 \pm$ ~~45~~45 MT CO_2/hour for October 25 for the 5-minute averaged data as shown.

Uncertainty in Q(t)

Seven measured parameters factor in to the emissions calculation of $Q(t)$for the two days. These are given in Table I along with the instrumental measurement precision and the observed variability. ~~In terms of instrument uncertainty, the precision of the retrieved CO_2 is 0.9 ppm for the reference path at our 30-second time resolution (Waxman et al., 2017) and 0.5 ppm for the over-city path. The precision is better over the longer path because the absorption lines are stronger~~ which improves our signal to noise, ~~but the precision does not improve linearly with path length because we have substantially lower light return over the 6.7 km path (see Section 2.1) which worsens our signal to noise.~~ Note that solar insolation is used solely in the determination of the Pasquill stability class (Seinfeld and Pandis, 2006). The stability class is relatively insensitive to the variations in solar insolation observed on the two test case days. As can be seen in the table, the uncertainty is dominated by the natural variability in parameters like wind speed, wind direction, and CO_2 concentration rather than the ~~instrument~~ DCS spectrometer precision. ~~The~~ observed variability over the 5-~~6~~9 hour period is typically at least a factor of 2 larger than the instrument precision. The variability in these parameters leads to the observed variability in $Q(t)$. We use the mean of $Q(t)$ as our emissions value and the ~~above quoted~~ standard deviation (at 5-~~-~~minute time-averaging) as its uncertainty. In using this standard deviation as a measure of the uncertainty, we attempt to capture the uncertainty associated with the discrepancies between, for example, the weather-station measurements of wind direction and speed relative to the true wind direction (which results in greater or fewer number of plumes from the given traffic locations intercepting the measurement path). This variability appears in $Q(t)$ as the nominal measured wind direction varies. Future systems with redundant, distributed DCS beam paths would provide a superior estimate of all these uncertainties.

In addition, there are assumptions, and possible uncertainties, inherent to the Gaussian plume model. ~~For example~~First, the model does not include the effects of buildings, trees, or other objects that could break up the plume between the emissions location and the beam path. Second, ~~W~~we ~~also~~ assume that all CO_2 emissions come from the discrete locations shown in Fig. 1, while in reality the emissions are likely substantially more diffuse. The assumption of discrete emissions simplifies modeling and is feasible due to the city traffic data~~,~~ but may result in a bias due to the coarse distribution of traffic measurements. Third, ~~W~~we approximate the measurement height at 15 m above ground although the beam height differs over the path since Boulder is not perfectly flat. Finally, we use standard I_y, J_y, K_y, I_z, J_z, and K_z values which were derived for rural areas (Turner, 1970) which may be different than urban or suburban areas. However, the greatest differences between rural and urban conditions are expected to be at night (Turner, 1970).

~~3.3.4 Scaling to annual emissions~~

~~In order to compare with the city inventory, our results must be scaled to an annual total. To do this, T~~~~t~~~~he Gaussian plume results are scaled to daily emissions using the hourly traffic data in Fig. 3. The traffic data in Fig. 3 comes from weekday measurements, but due to the lack of available weekend data we assume that the distribution is the same for weekends. Based on these data, 33% of the total traffic counts on Oct. 22 occur during the 5-hour measurement period and 39% of the total traffic counts on Oct. 25 occur during the 6-hour measurement period. Then we scale to annual emissions by assuming that the emissions on Oct. 22 are representative of all 104 weekend days and the emissions on Oct. 25 are representative of all 261 week days. Scaling the mean values of in this way, we estimate an annual emission rate of MT CO_2/year. The uncertainty is simply the scaled variability in the measured and does not include additional uncertainty from scaling to annual emissions or the use of TMC data as a proxy for emissions locations.~~

3.3.3~~45~~ Corrections for non-traffic sources of CO_2

There are a number of non-traffic sources of CO_2 that could contribute to our measured X_{CO2} enhancement including local power plants, residential emission, and biological activity. These non-traffic source should have relatively minor contribution for several~~two~~ reasons. First, the footprint of the over-city path does not overlap the large power plant to the east of the Boulder city limits. Secon~~-First~~d, the temperature during the two test case days ~~ranged from XXx to y25~~was 24 °C and 20 °C (68 °F~~z~~ and~~to~~ ~~f75~~7 °F) on October 22 and 25th leading to minimal residential and commercial heating. Third~~Second~~, the measurements ~~two test case days~~ occurred in October after leaf senescence so there should be negligible biological activity. ~~, as discussed before.~~ Nevertheless, as discussed below, we do ~~make corrections~~adjust ~~to~~ our measurements to account for the relatively minor contribution from non-traffic sources before scaling up to an estimate of the annual traffic emissions.

We first consider power plants. There are ~~the~~ two power generation facilities on the Department of Commerce (DOC) campus ~~and collocated with NIST~~ located near the NIST building that houses the dual-comb spectrometer: the site's Central Utilities Plant (CUP), and the National Oceanic and Atmospheric Administration (NOAA) building's ~~NOAA~~ boilers. To calculate their average CO_2 emissions, we used available fuel consumption data (October 2016 monthly average for the CUP and mid-November to mid-December 2016 average for the NOAA boilers; October data was unavailable) and the EPA emissions factor (EPA, 1995). We then modeled the CUP and boiler plume emissions using WindTrax (Flesch et al., 1995, 2004) with wind speed and direction data from the NCAR-Mesa site. We find that due to the moderate wind speeds (~~>~~5 m/s) during our case study days and the height mismatch between the emission stacks and our measurement path over the DOC campus, there ~~should be~~is negligible enhancement over the reference path. Given the location of the emission sources and the wind direction during our measurement periods, the emissions also~~y~~ do not cross the over-city beam path ~~either~~. Therefore, we apply no correction for these two power plant emissions.

~~It is also possible that emissions from t~~The University of Colorado also has a power plant that falls within the main footprint associated with the over-city beam path, shown in Fig. 7a, and ~~therefore~~ whose emissions ~~are expected to~~could intersect our over-city beam path. The EPA Greenhouse Gas Reporting Program (GHGRP, https://www.epa.gov/ghgreporting) lists the 201~~7~~6 emission from the power plant as 2~~3~~.~~0~~7 × 10^4 MT~~/year~~ CO_2 or an average of 3.1 MT/hour. (No breakdown by season or hour is provided.) We~~, which is approximately 5% of our calculated emissions value and thus not a significant bias given our large uncertainty. If we account for the CO_2 from this power plant then our annual vehicle emissions estimate is reduced slightly to MT/year~~ apply this correction to our previous daily values and add a conservative~~n~~ uncertainty equal to this correction in quadrature with the previous uncertainty. The new adjusted values are then 28 ± 17 MT CO_2/hour for October 22 and 162 ± 4~~2~~5 MT CO_2/hour for October 25. ~~.~~

The~~A~~ large Valmont power station ~~power plant~~ lies just outside the city limits to the east of Boulder ~~(the Valmont power station);~~ ; however, given its location and the dominant westerly wind, emissions from this source ~~should~~ does not reach our beam path~~s~~. There are no other power generation facilities within the city that report to the GHGRP, so we make no further corrections based on power plants. ~~likely~~

~~Of course, other small power generation facilities exist within the city that do not report to the GHGRP but may still produce emissions that intersect our beam path that we are unable to account for.~~

~~Certainly, t~~ In addition, ~~T~~there are also likely diffuse emissions from residential and commercial furnaces and water heaters that use natural gas. The City of Boulder Community Greenhouse Gas Emissions Inventory reports twenty percent of the city emissions, or 3.18×10^5 MT CO2e, were from natural gas in 2016 (https://www-static.bouldercolorado.gov/docs/2016_Greenhouse_Gas_Emissions_Inventory_Report_FINAL-1-201803121328.pdf?_ga=2.130927943.970967930.1525795820-107394975). The natural gas usage varies strongly by month with building heating requirements. Although our measurements occurred in October, ~~However, as discussed above (in Section 22),~~ the measurement days were quite warm (20-24 C) ~~heaters~~

~~were running during the measurement time period~~so that residential and commercial building heating was unlikely and the use of an annual average would overestimate any contribution. Instead, we scale the natural gas usage according to the monthly breakdown provided by the United States Energy Information Administration database for Colorado ~~occurred during the October 2016~~ (https://www.eia.gov/dnav/ng/hist/n3010co2m.htm). The mean daytime (approximately sunrise to sunset, 7 am to 6 pm) temperature in October was 18.2 C while the mean temperature (including day and night) for October was 15.7 C. Our daytime-only measurements therefore had a mean temperature that was much closer to the mean temperature (day and night) of September, which was 19.2 C. Therefore, we scale the Boulder annual natural gas consumption by ~~, we redo the above correct~~the September 2016 nature gas usage, ~~natural gas usage data,~~ which was 2.~~4~~6% of the Colorado annual total according ~~occurred during the October 2016 (~~https://www.eia.gov/dnav/ng/hist/n3010co2m.htm). ~~natural gas usage in Colorado.~~The estimated total emissions from residential and commercial natural gas usage in Boulder over our measurement days is then 10.2 MT CO_2~~e~~/hour. We apply this correction to our measured values and include a (conservative) uncertainty equal to this correction. The new adjusted values are then $Q_{Oct22,adj}$ = 18 ± 20 MT CO_2/hour for October 22 and $Q_{Oct25,adj}$ = 152 ± ~~46~~27 MT CO_2/hour for October 25.

Once leaf senescence has completed, neither plants nor soil respiration contribute to CO_2 signal (Matyssek et al., 2013). The National Phenology Network (USA National Phenology Network, 2018) data shows that for the site nearest to Boulder (64 km north of Boulder), the leaf fall dates were September 15, 2016 for box elder trees October 6, 2016 for Eastern cottonwoods. T~~ and t~~hus by our measurement dates leaf senescence should be fully complete and plants will not contribute to the city CO_2 enhancement. We note that a wide range of biogenic contributions to CO_2 have been noted in the literature (Gurney et al., 2017; Mitchell et al., 2018; Sargent et al., 2018)~~(Gurney et al., 2017) {Citation} (Mitchell et al., 2018) reports. We likely also measure contributions from plant and soil respiration as these measurements were made in the late fall when photosynthesis was likely minimal but respiration was likely ongoing because the temperatures were above freezing. Respiration was found to be a significant source of CO_2 emissions in Indianapolis (Gurney et al., 2017). As with the emissions from furnaces or smaller generation facilities, we have not attempted to quantify or correct for this effect, which could inflate our estimate.~~

3.3.4~~5~~ Scaling to annual emissions

In order to compare with the city inventory, we scale our results to an annual total. To do this, we use the hourly traffic data of Fig. 4 to ~~scale our two measurement windows~~scale $Q_{Oct22,adj}$ and $Q_{Oct25,adj}$ to a daily emission~~3~~. Based on Figure 4, 3~~3~~4% of the total traffic counts occur during the 5-hour measurement period on Oct. 22 and ~~39~~52~~58~~% of the total traffic counts occur during the ~~6~~8-hour measurement period on Oct. 25 (excluding the 13:00 to 14:00 period). The daily emissions are then $Q_{Oct22,day} = Q_{Oct22,adj} \times (5 \text{ hours}) \div (0.34)$ and $Q_{Oct25,day} = Q_{Oct25,adj} \times (8 \text{ hours}) \div (0.52)$ ((~~The traffic data in Fig. 4~~3 is based on weekday measurement and we ~~must~~ assume that the hourly distribution is the same for weekends; ~~.~~this may lead to a slight overestimate in the weekend data where a larger fraction of emissions occurs between 11 am and 4 pm than on weekdays.) ~~Then w~~We then scale to annual emissions by assuming that the emissions on Oct. 22 are representative of all 112 weekend/holiday days and the emissions on Oct. 25 are representative of all 253 work~~-~~days. Including their uncertainty, this calculation yields $(6.2 \pm 1.8) \times 10^5$ MT CO_2/year.

The scaling relies heavily on the traffic count data supplied by the city of Boulder, which does not have an associated uncertainty value. A comparison of these data over several years shows a typical 7% statistical variation at a given TMC location, after removing a linear trend. We assume this reflects day-to-day fluctuations in traffic. In addition, there will be seasonal variations, which is not captured in the extrapolation from our two test case days to the annual emissions. Due to the lack of seasonal data for Boulder traffic, we use the detailed Hestia traffic inventory for Salt Lake City, UT given in Figure 2 of (Mitchell et al., 2018)~~(Mitchell et al., 2018)~~. These data show a variation of ±18% in traffic emissions between "summer" and "winter" months. Combined in quadrature with the 7% statistical uncertainty in the TMC traffic count data, this leads to an additional ~20% uncertainty to the scaled annual estimate. As

noted earlier, we have not applied any additional uncertainty on the reliance on the TMC data as a proxy for emissions locations.

Including the additional uncertainty on the scaling to annual emissions, we estimate~~Scaling the corrected mean values of $Q(t)$ and their uncertainties in this way, we estimate~~ an annual emission rate of (6.2~~0~~ ± 2~~1~~.~~11~~2) × 10^5 MT CO_2/year for traffic carbon emissions for Boulder CO.

~~.~~

~~The uncertainty is simply the scaled variability in the measured and does not include additional uncertainty from scaling to annual emissions or the use of TMC data as a proxy for emissions locations. <The count uncertainty is about 7% at most based on looking at the data, the seasonal uncertainty of October versus other days just scales all the numbers up and down so it does not matter, so the uncertainty is really based on the area coverage or essentially inventory maybe put that all down in there.>~~

~~*Uncertainty in the scaling to city-wide annual emissions*~~

~~Values supplied by the city of Boulder traffic count data and emissions inventory numbers do not have an associated uncertainty value. However, even if there was negligible uncertainty on the measurements, there is inherent statistical uncertainty in the strong extrapolation from our 5-96 hour period to a full day and then to the entire year. Moreover, the traffic data used to scale the emissions up from 6 hours to 24 hours was collected solely on week days, which might lead to a slight overestimate in the weekend data because a larger fraction of the weekend emissions occur between 11 am and 4 pm than weekday emissions. Obviously, the extrapolation also misses seasonality in the emissions. Further, implicitly built in to Equation 4 is a spatial scaling that uses discrete points from a subsection of the city (those emissions locations whose beam paths cross our measurement path). The systematic uncertainty in this spatial and temporal scaling from our measurements to annual city emissions is unknown but possibly substantial. Without additional information, it is not possible to add additional uncertainty to the current 26% uncertainty, which is based solely on the measured variability in $Q(t)$.~~

4 Comparison with city estimates

The c~~C~~ity vehicle emissions estimate comes from total vehicle miles traveled based on data from the t~~T~~ransportation department, miles per gallon inputs from the EPA state inventory tool, and vehicle type distribution from the Colorado Department of Public Health and the Environment (Kimberlee Rankin, City of Boulder, personal communication).The City of Boulder estimates ~~that the~~ total vehicle emissions of ~~were 4.47x10^5~~ 4.50~~x~~×10^5 metric tons (MT) of CO_2 ~~equivalent (CO_2e)~~ in 201~~5~~6, ~~the most recent year of the city greenhouse gas inventory. When scaled up to 2016 levels based on total vehicle miles traveled (8.98x10^8 miles in 2015 and 9.09x10^8 miles in 2016), this is 4.52x10^5 MT CO_2e in 2016~~ (https://www-static.bouldercolorado.gov/docs/2016_Greenhouse_Gas_Emissions_Inventory_Report_FINAL-1-201803121328.pdf?_ga=2.130927943.970967930.1525795820-107394975). On-road emissions account for greater than 99% of the transportation emissions, so we have scaled this value down by one percent for an on-road emissions value of 4.46~~5~~×~~x~~10^5 MT CO_2. We assume that all traffic emissions are CO_2 rather than a mix of CO_2 and CH_4. There is no uncertainty provided by the city on this value.

In comparison, we estimate (6.2 ± 2.2) × 10^5 MT CO_2/year MT CO_2/year, which is 13955% of the city estimate but agrees within the given uncertainty. Interestingly, ~~While the discrepancy is moderately large it is reasonable agreement for a top-down measurement and bottom-up inventory comparison, especially given that there are possibly additional CO_2 sources contributing to our measured values that we are currently unable to quantify.~~ o~~O~~ther studies have also found that emissions measurements were higher than the reported inventory values. Brioude et al., (2013) found top-down aircraft estimates of Los Angeles county and the South Coast Air Basin (SoCAB) CO_2 were 1.45 times larger than the Vulcan 2005 inventory (Gurney et al., 2009). An earlier aircraft campaign over Sacramento, CA found an average CO_2 emission, with 100% uncertainty, that was 15-20% higher than the Vulcan estimate (Turnbull et al., 2011). Lauvaux et al. (2016) compared Indianapolis city CO_2 emissions measured by a

network of CRDS instruments to the HESTIA inventory (Gurney et al., 2012) during INFLUX (Davis et al., 2017). They found that despite the building-scale resolution in the HESTIA inventory, it still underestimated the annual CO_2 flux by 20%. An updated version of HESTIA predicted very similar emissions estimates for on-road, residential, and commercial sectors, so the discrepancy was attributed to missing sources of CO_2, including animal (primarily human and companion animal) respiration, biofuel combustion, and biosphere respiration (Gurney et al., 2017).

4.1 Improvements in future measurements

Future improvements should include additional and different beam paths, selected based on prevailing wind directions. (Our initial assumption that the mountain path would generally act as a reference path was incorrect since the prevailing daytime winds are not out of the west but rather the southeast.) An east-west running beam north of the city and one south of the city would allow us to utilize a larger fraction of the data as the predominant midday wind direction during the fall is out of the north to north-east (see Fig. 15). Even longer beam paths would also interrogate a larger fraction of the city and measure a correspondingly larger fraction of the vehicle emissions. Vertically-resolved data from e.g. a series of stacked retroreflectors would better test the assumption of vertically-dispersing Gaussian plumes.

Additionally, more extensive modeling to cover variable wind directions and speeds would allow the incorporation of a much larger fraction of the data than the two days selected here. An inversion-based model similar to (Lauvaux et al., 2013) could potentially be applied to a small city like Boulder; however this would depend heavily on the quality of the bottom-up emissions inventory used to generate the priors. Indeed, one of the major future improvements would be to generate a detailed Hestia inventory of Boulder, CO similar to that generated for Salt Lake City, UT (Mitchell et al., 2018).

5 Conclusions

We demonstrate the use of an open-path dual frequency comb spectroscopy system for quantifying city emissions of carbon dioxide. We send light over two paths: a reference path that samples the concentration of gases entering the city from the west, and an over-city path that measures the concentrations of gases after the air mass has crossed approximately two-thirds of the city including two major commuter arteries. The measured diurnal cycle shows a significant ~~commuter peak~~traffic-related enhancement in the carbon dioxide signal during weekdays in the over-city path compared to the reference path. We select two case study days with appropriate wind conditions and apply Gaussian plume modeling to estimate the total vehicular carbon emission. We then scale these results up to annual city-wide emissions using traffic data from the City of Boulder. We find overall traffic related carbon emissions that are approximately 1.3945 times greater than the city's bottom-up traffic emissions inventory but with an uncertainty that encompasses the city inventory estimate. ~~This is reasonably good agreement given the limited number of measurement days that were suitable for the modeling and assumptions in the use of a Gaussian plume model.~~ Further improvements to this method should include improved design of reference and over-city paths~~, enabling this method to be used for multiple wind directions.~~ and a more detailed inventory model for Boulder CO, which together should further reduce the overall uncertainty in the estimate.

Acknowledgements: We thank Kimberlee Rankin, Randall Rutsch, Bill Cowern, and Chris Hagelin from the City of Boulder for city inventory and traffic information and Dave Plusquellic and Caroline Alden for assistance with the manuscript. This work was funded by Defense Advanced Research Program Agency DSO SCOUT program, and James Whetstone and the NIST special program office. Eleanor M. Waxman and Kevin C. Cossel are partially supported by National Research Council postdoctoral fellowships.

5. References

Bergeron, O. and Strachan, I. B.: CO_2 sources and sinks in urban and suburban areas of a northern mid-latitude city, Atmos. Environ., 45(8), 1564–1573, doi:10.1016/j.atmosenv.2010.12.043, 2011.

Bréon, F. M., Broquet, G., Puygrenier, V., Chevallier, F., Xueref-Remy, I., Ramonet, M., Dieudonné, E., Lopez, M., Schmidt, M., Perrussel, O. and Ciais, P.: An attempt at estimating Paris area CO_2 emissions from atmospheric concentration measurements, Atmos Chem Phys, 15(4), 1707–1724, doi:10.5194/acp-15-1707-2015, 2015.

Brioude, J., Angevine, W. M., Ahmadov, R., Kim, S.-W., Evan, S., McKeen, S. A., Hsie, E.-Y., Frost, G. J., Neuman, J. A., Pollack, I. B., Peischl, J., Ryerson, T. B., Holloway, J., Brown, S. S., Nowak, J. B., Roberts, J. M., Wofsy, S. C., Santoni, G. W., Oda, T. and Trainer, M.: Top-down estimate of surface flux in the Los Angeles Basin using a mesoscale inverse modeling technique: assessing anthropogenic emissions of CO, NO_x and CO_2 and their impacts, Atmos Chem Phys, 13(7), 3661–3677, doi:10.5194/acp-13-3661-2013, 2013.

Ciais, P., Rayner, P., Chevallier, F., Bousquet, P., Logan, M., Peylin, P. and Ramonet, M.: Atmospheric inversions for estimating CO_2 fluxes: methods and perspectives, Clim. Change, 103(1–2), 69–92, doi:10.1007/s10584-010-9909-3, 2010.

Coburn, S., Alden, C. B., Wright, R., Cossel, K., Baumann, E., Truong, G.-W., Giorgetta, F., Sweeney, C., Newbury, N. R., Prasad, K., Coddington, I. and Rieker, G. B.: Regional trace-gas source attribution using a field-deployed dual frequency comb spectrometer, Optica, 5(4), 320–327, doi:10.1364/OPTICA.5.000320, 2018.

Coddington, I., Newbury, N. and Swann, W.: Dual-comb spectroscopy, Optica, 3(4), 414, doi:10.1364/OPTICA.3.000414, 2016.

Cossel, K. C., Waxman, E. M., Giorgetta, F. R., Cermak, M., Coddington, I. R., Hesselius, D., Ruben, S., Swann, W. C., Truong, G.-W., Rieker, G. B. and Newbury, N. R.: Open-path dual-comb spectroscopy to an airborne retroreflector, Optica, 4(7), 724–728, doi:10.1364/OPTICA.4.000724, 2017.

Coutts, A. M., Beringer, J. and Tapper, N. J.: Characteristics influencing the variability of urban CO_2 fluxes in Melbourne, Australia, Atmos. Environ., 41(1), 51–62, doi:10.1016/j.atmosenv.2006.08.030, 2007.

Davis, K. J., Deng, A., Lauvaux, T., Miles, N. L., Richardson, S. J., Sarmiento, D. P., Gurney, K. R., Hardesty, R. M., Bonin, T. A., Brewer, W. A., Lamb, B. K., Shepson, P. B., Harvey, R. M., Cambaliza, M. O., Sweeney, C., Turnbull, J. C., Whetstone, J. and Karion, A.: The Indianapolis Flux Experiment (INFLUX): A test-bed for developing urban greenhouse gas emission measurements, Elem Sci Anth, 5(0), 21, doi:10.1525/elementa.188, 2017.

Dobler, J. T., Zaccheo, T. S., Pernini, T. G., Blume, N., Broquet, G., Vogel, F., Ramonet, M., Braun, M., Staufer, J., Ciais, P. and Botos, C.: Demonstration of spatial greenhouse gas mapping using laser absorption spectrometers on local scales, J. Appl. Remote Sens., 11(1), 014002, doi:10.1117/1.JRS.11.014002, 2017.

EPA: AP 42, Fifth Edition Compilation of Air Pollutant Emissions Factors, Volume 1: Stationary Point and Area Sources, [online] Available from: https://www.epa.gov/air-emissions-factors-and-quantification/ap-42-compilation-air-emission-factors#5thed, 1995.

Fasoli, B., Lin, J. C., Bowling, D. R., Mitchell, L. and Mendoza, D.: Simulating atmospheric tracer concentrations for spatially distributed receptors: updates to the Stochastic Time-Inverted Lagrangian Transport model's R interface (STILT-R version 2), Geosci. Model Dev., 11(7), 2813–2824, doi:https://doi.org/10.5194/gmd-11-2813-2018, 2018.

Flesch, T. K., Wilson, J. D. and Yee, E.: Backward-Time Lagrangian Stochastic Dispersion Models and Their Application to Estimate Gaseous Emissions, J. Appl. Meteorol., 34(6), 1320–1332, doi:10.1175/1520-0450(1995)034<1320:BTLSDM>2.0.CO;2, 1995.

Flesch, T. K., Wilson, J. D., Harper, L. A., Crenna, B. P. and Sharpe, R. R.: Deducing Ground-to-Air Emissions from Observed Trace Gas Concentrations: A Field Trial, J. Appl. Meteorol., 43(3), 487–502, doi:10.1175/1520-0450(2004)043<0487:DGEFOT>2.0.CO;2, 2004.

Gurney, K. R., Mendoza, D. L., Zhou, Y., Fischer, M. L., Miller, C. C., Geethakumar, S. and Du Can, S. D. L. R.: High Resolution Fossil Fuel Combustion CO_2 Emission Fluxes for the United States, Environ. Sci. Technol., 43(14), 5535–5541, doi:10.1021/es900806c, 2009.

Gurney, K. R., Razlivanov, I., Song, Y., Zhou, Y., Benes, B. and Abdul-Massih, M.: Quantification of Fossil Fuel CO_2 Emissions on the Building/Street Scale for a Large U.S. City, Environ. Sci. Technol., 46(21), 12194–12202, doi:10.1021/es3011282, 2012.

Gurney, K. R., Liang, J., Patarasuk, R., O'Keeffe, D., Huang, J., Hutchins, M., Lauvaux, T., Turnbull, J. C. and Shepson, P. B.: Reconciling the differences between a bottom-up and inverse-estimated $FFCO_2$ emissions estimate in a large US urban area, Elem Sci Anth, 5(0), doi:10.1525/elementa.137, 2017.

Hedelius, J. K., Liu, J., Oda, T., Maksyutov, S., Roehl, C. M., Iraci, L. T., Podolske, J. R., Hillyard, P. W., Liang, J., Gurney, K. R., Wunch, D. and Wennberg, P. O.: Southern California megacity CO_2, CH_4, and CO flux estimates using ground- and space-based remote sensing and a Lagrangian model, Atmospheric Chem. Phys., 18(22), 16271–16291, doi:https://doi.org/10.5194/acp-18-16271-2018, 2018.

Heimburger, A. M. F., Harvey, R. M., Shepson, P. B., Stirm, B. H., Gore, C., Turnbull, J., Cambaliza, M. O. L., Salmon, O. E., Kerlo, A.-E. M., Lavoie, T. N., Davis, K. J., Lauvaux, T., Karion, A., Sweeney, C., Brewer, W. A., Hardesty, R. M. and Gurney, K. R.: Assessing the optimized precision of the aircraft mass balance method for measurement of urban greenhouse gas emission rates through averaging, Elem Sci Anth, 5(0), doi:10.1525/elementa.134, 2017.

Hendrick, M. F., Ackley, R., Sanaie-Movahed, B., Tang, X. and Phillips, N. G.: Fugitive methane emissions from leak-prone natural gas distribution infrastructure in urban environments, Environ. Pollut., 213, 710–716, doi:10.1016/j.envpol.2016.01.094, 2016.

Jackson, R. B., Down, A., Phillips, N. G., Ackley, R. C., Cook, C. W., Plata, D. L. and Zhao, K.: Natural Gas Pipeline Leaks Across Washington, DC, Environ. Sci. Technol., 48(3), 2051–2058, doi:10.1021/es404474x, 2014.

Järvi, L., Rannik, Ü., Kokkonen, T. V., Kurppa, M., Karppinen, A., Kouznetsov, R. D., Rantala, P., Vesala, T. and Wood, C. R.: Uncertainty of eddy covariance flux measurements over an urban area based on two towers, Atmospheric Meas. Tech., 11(10), 5421–5438, doi:https://doi.org/10.5194/amt-11-5421-2018, 2018.

Lamb, B. K., Cambaliza, M. O. L., Davis, K. J., Edburg, S. L., Ferrara, T. W., Floerchinger, C., Heimburger, A. M. F., Herndon, S., Lauvaux, T., Lavoie, T., Lyon, D. R., Miles, N., Prasad, K. R.,

Richardson, S., Roscioli, J. R., Salmon, O. E., Shepson, P. B., Stirm, B. H. and Whetstone, J.: Direct and Indirect Measurements and Modeling of Methane Emissions in Indianapolis, Indiana, Environ. Sci. Technol., 50(16), 8910–8917, doi:10.1021/acs.est.6b01198, 2016.

Lauvaux, T., Miles, N. L., Richardson, S. J., Deng, A., Stauffer, D. R., Davis, K. J., Jacobson, G., Rella, C., Calonder, G.-P. and DeCola, P. L.: Urban Emissions of CO_2 from Davos, Switzerland: The First Real-Time Monitoring System Using an Atmospheric Inversion Technique, J. Appl. Meteorol. Climatol., 52(12), 2654–2668, doi:10.1175/JAMC-D-13-038.1, 2013.

Lauvaux, T., Miles, N. L., Deng, A., Richardson, S. J., Cambaliza, M. O., Davis, K. J., Gaudet, B., Gurney, K. R., Huang, J., O'Keefe, D., Song, Y., Karion, A., Oda, T., Patarasuk, R., Razlivanov, I., Sarmiento, D., Shepson, P., Sweeney, C., Turnbull, J. and Wu, K.: High-resolution atmospheric inversion of urban CO_2 emissions during the dormant season of the Indianapolis Flux Experiment (INFLUX), J. Geophys. Res. Atmospheres, 121(10), 2015JD024473, doi:10.1002/2015JD024473, 2016.

Marcotullio, P. J., Sarzynski, A., Albrecht, J., Schulz, N. and Garcia, J.: The geography of global urban greenhouse gas emissions: an exploratory analysis, Clim. Change, 121(4), 621–634, doi:10.1007/s10584-013-0977-z, 2013.

Matyssek, R., Clarke, N., Cudlin, P., Mikkelsen, T. N., Tuovinen, J.-P., Wieser, G. and Paoletti, E.: Climate Change, Air Pollution and Global Challenges: Understanding and Perspectives from Forest Research, Elsevier, London, UNITED KINGDOM. [online] Available from: http://ebookcentral.proquest.com/lib/noaalabs-ebooks/detail.action?docID=1568332 (Accessed 19 December 2018), 2013.

Mays, K. L., Shepson, P. B., Stirm, B. H., Karion, A., Sweeney, C. and Gurney, K. R.: Aircraft-Based Measurements of the Carbon Footprint of Indianapolis, Environ. Sci. Technol., 43(20), 7816–7823, doi:10.1021/es901326b, 2009.

McKain, K., Wofsy, S. C., Nehrkorn, T., Eluszkiewicz, J., Ehleringer, J. R. and Stephens, B. B.: Assessment of ground-based atmospheric observations for verification of greenhouse gas emissions from an urban region, Proc. Natl. Acad. Sci., 109(22), 8423–8428, doi:10.1073/pnas.1116645109, 2012.

McKain, K., Down, A., Raciti, S. M., Budney, J., Hutyra, L. R., Floerchinger, C., Herndon, S. C., Nehrkorn, T., Zahniser, M. S., Jackson, R. B., Phillips, N. and Wofsy, S. C.: Methane emissions from natural gas infrastructure and use in the urban region of Boston, Massachusetts, Proc. Natl. Acad. Sci., 112(7), 1941–1946, doi:10.1073/pnas.1416261112, 2015.

Mitchell, L. E., Lin, J. C., Bowling, D. R., Pataki, D. E., Strong, C., Schauer, A. J., Bares, R., Bush, S. E., Stephens, B. B., Mendoza, D., Mallia, D., Holland, L., Gurney, K. R. and Ehleringer, J. R.: Long-term urban carbon dioxide observations reveal spatial and temporal dynamics related to urban characteristics and growth, Proc. Natl. Acad. Sci., 115(12), 2912–2917, doi:10.1073/pnas.1702393115, 2018.

Mueller, K., Yadav, V., Lopez-Coto, I., Karion, A., Gourdji, S., Martin, C. and Whetstone, J.: Siting background towers to characterize incoming air for urban greenhouse gas estimation: a case study in the Washington DC/Baltimore Area, J. Geophys. Res. Atmospheres, 2017JD027364, doi:10.1002/2017JD027364, 2017.

Nemitz, E., Hargreaves, K. J., McDonald, A. G., Dorsey, J. R. and Fowler, D.: Micrometeorological Measurements of the Urban Heat Budget and CO_2 Emissions on a City Scale, Environ. Sci. Technol., 36(14), 3139–3146, doi:10.1021/es010277e, 2002.

Phillips, N. G., Ackley, R., Crosson, E. R., Down, A., Hutyra, L. R., Brondfield, M., Karr, J. D., Zhao, K. and Jackson, R. B.: Mapping urban pipeline leaks: Methane leaks across Boston, Environ. Pollut., 173(Supplement C), 1–4, doi:10.1016/j.envpol.2012.11.003, 2013.

Prussin, A. J., Marr, L. C., Schmale, D. G., Stoll, R. and Ross, S. D.: Experimental validation of a long-distance transport model for plant pathogens: Application to Fusarium graminearum, Agric. For. Meteorol., 203, 118–130, doi:10.1016/j.agrformet.2014.12.009, 2015.

Rieker, G. B., Giorgetta, F. R., Swann, W. C., Kofler, J., Zolot, A. M., Sinclair, L. C., Baumann, E., Cromer, C., Petron, G., Sweeney, C., Tans, P. P., Coddington, I. and Newbury, N. R.: Frequency-comb-based remote sensing of greenhouse gases over kilometer air paths, Optica, 1(5), 290–298, doi:10.1364/OPTICA.1.000290, 2014.

Rothman, L. S., Gordon, I. E., Barbe, A., Benner, D. C., Bernath, P. E., Birk, M., Boudon, V., Brown, L. R., Campargue, A., Champion, J. P., Chance, K., Coudert, L. H., Dana, V., Devi, V. M., Fally, S., Flaud, J. M., Gamache, R. R., Goldman, A., Jacquemart, D., Kleiner, I., Lacome, N., Lafferty, W. J., Mandin, J. Y., Massie, S. T., Mikhailenko, S. N., Miller, C. E., Moazzen-Ahmadi, N., Naumenko, O. V., Nikitin, A. V., Orphal, J., Perevalov, V. I., Perrin, A., Predoi-Cross, A., Rinsland, C. P., Rotger, M., Simeckova, M., Smith, M. A. H., Sung, K., Tashkun, S. A., Tennyson, J., Toth, R. A., Vandaele, A. C. and Vander Auwera, J.: The HITRAN 2008 molecular spectroscopic database, J. Quant. Spectrosc. Radiat. Transf., 110(9–10), 533–572, doi:10.1016/j.jqsrt.2009.02.013, 2009.

Ryerson, T. B., Trainer, M., Holloway, J. S., Parrish, D. D., Huey, L. G., Sueper, D. T., Frost, G. J., Donnelly, S. G., Schauffler, S., Atlas, E. L., Kuster, W. C., Goldan, P. D., Hübler, G., Meagher, J. F. and Fehsenfeld, F. C.: Observations of Ozone Formation in Power Plant Plumes and Implications for Ozone Control Strategies, Science, 292(5517), 719–723, doi:10.1126/science.1058113, 2001.

Sargent, M., Barrera, Y., Nehrkorn, T., Hutyra, L. R., Gately, C. K., Jones, T., McKain, K., Sweeney, C., Hegarty, J., Hardiman, B., Wang, J. A. and Wofsy, S. C.: Anthropogenic and biogenic CO_2 fluxes in the Boston urban region, Proc. Natl. Acad. Sci., 115(29), 7491–7496, doi:10.1073/pnas.1803715115, 2018.

Seinfeld, J. H. and Pandis, S. N.: Atmospheric Chemistry and Physics: From Air Pollution to Climate Change, Wiley., 2006.

Seto, K. C., Bigio, A., Bento, A., Cervero, R. and Christensen, P.: Human Settlements, Infrastructure, and Spatial Planning, in Climate Change 2014: Mitigation of Climate Change. Contribution of Working Group III to the Fifth Assessment Report of the Intergovernmental Panel on Climate Change, p. 78., 2014.

Shusterman, A. A., Teige, V. E., Turner, A. J., Newman, C., Kim, J. and Cohen, R. C.: The BErkeley Atmospheric CO_2 Observation Network: initial evaluation, Atmos Chem Phys, 16(21), 13449–13463, doi:10.5194/acp-16-13449-2016, 2016.

Staufer, J., Broquet, G., Bréon, F.-M., Puygrenier, V., Chevallier, F., Xueref-Rémy, I., Dieudonné, E., Lopez, M., Schmidt, M., Ramonet, M., Perrussel, O., Lac, C., Wu, L. and Ciais, P.: The first 1-year-long estimate of the Paris region fossil fuel CO_2 emissions based on atmospheric inversion, Atmos Chem Phys, 16(22), 14703–14726, doi:10.5194/acp-16-14703-2016, 2016.

Truong, G.-W., Waxman, E. M., Cossel, K. C., Baumann, E., Klose, A., Giorgetta, F. R., Swann, W. C., Newbury, N. R. and Coddington, I.: Accurate frequency referencing for fieldable dual-comb spectroscopy, Opt. Express, 24(26), 30495–30504, doi:10.1364/OE.24.030495, 2016.

Turnbull, J. C., Karion, A., Fischer, M. L., Faloona, I., Guilderson, T., Lehman, S. J., Miller, B. R., Miller, J. B., Montzka, S., Sherwood, T., Saripalli, S., Sweeney, C. and Tans, P. P.: Assessment of fossil fuel carbon dioxide and other anthropogenic trace gas emissions from airborne measurements over Sacramento, California in spring 2009, Atmos Chem Phys, 11(2), 705–721, doi:10.5194/acp-11-705-2011, 2011.

Turner, D. B.: Workbook of Atmospheric Dispersion Estimates, [online] Available from: https://ia802704.us.archive.org/4/items/workbookofatmosp026353mbp/workbookofatmosp026353mbp.pdf (Accessed 5 June 2017), 1970.

USA National Phenology Network. 2018. Plant and Animal Phenology Data. Data type: Site Pheometrics. 09/01/2016-11/31/2016 for Region: Colorado. USA-NPN, Tucson, Arizona, USA. Data set accessed 12/18/2018 at http://doi.org/10.5066/F78S4N1

Velasco, E., Pressley, S., Allwine, E., Westberg, H. and Lamb, B.: Measurements of CO_2 fluxes from the Mexico City urban landscape, Atmos. Environ., 39(38), 7433–7446, doi:10.1016/j.atmosenv.2005.08.038, 2005.

Velasco, E., Perrusquia, R., Jiménez, E., Hernández, F., Camacho, P., Rodríguez, S., Retama, A. and Molina, L. T.: Sources and sinks of carbon dioxide in a neighborhood of Mexico City, Atmos. Environ., 97(Supplement C), 226–238, doi:10.1016/j.atmosenv.2014.08.018, 2014.

Verhulst, K. R., Karion, A., Kim, J., Salameh, P. K., Keeling, R. F., Newman, S., Miller, J., Sloop, C., Pongetti, T., Rao, P., Wong, C., Hopkins, F. M., Yadav, V., Weiss, R. F., Duren, R. M. and Miller, C. E.: Carbon dioxide and methane measurements from the Los Angeles Megacity Carbon Project – Part 1: calibration, urban enhancements, and uncertainty estimates, Atmos Chem Phys, 17(13), 8313–8341, doi:10.5194/acp-17-8313-2017, 2017.

Waxman, E. M., Cossel, K. C., Truong, G.-W., Giorgetta, F. R., Swann, W. C., Coburn, S., Wright, R. J., Rieker, G. B., Coddington, I. and Newbury, N. R.: Intercomparison of open-path trace gas measurements with two dual-frequency-comb spectrometers, Atmos Meas Tech, 10(9), 3295–3311, doi:10.5194/amt-10-3295-2017, 2017.

White, W. H., Anderson, J. A., Blumenthal, D. L., Husar, R. B., Gillani, N. V., Husar, J. D. and Wilson, W. E.: Formation and transport of secondary air pollutants: ozone and aerosols in the St. Louis urban plume, Science, 194(4261), 187–189, doi:10.1126/science.959846, 1976.

Wong, C. K., Pongetti, T. J., Oda, T., Rao, P., Gurney, K. R., Newman, S., Duren, R. M., Miller, C. E., Yung, Y. L. and Sander, S. P.: Monthly trends of methane emissions in Los Angeles from 2011 to 2015 inferred by CLARS-FTS observations, Atmos Chem Phys, 16(20), 13121–13130, doi:10.5194/acp-16-13121-2016, 2016.

Wong, K. W., Fu, D., Pongetti, T. J., Newman, S., Kort, E. A., Duren, R., Hsu, Y.-K., Miller, C. E., Yung, Y. L. and Sander, S. P.: Mapping CH_4 : CO_2 ratios in Los Angeles with CLARS-FTS from Mount Wilson, California, Atmospheric Chem. Phys., 15(1), 241–252, doi:https://doi.org/10.5194/acp-15-241-2015, 2015.

Wunch, D., Wennberg, P. O., Toon, G. C., Keppel-Aleks, G. and Yavin, Y. G.: Emissions of greenhouse gases from a North American megacity, Geophys. Res. Lett., 36(15), L15810, doi:10.1029/2009GL039825, 2009.

Wunch, D., Toon, G. C., Sherlock, V., Deutscher, N. M., Liu, C., Feist, D. G. and Wennberg, P. O.: Documentation for the 2014 TCCON Data Release, , doi:10.14291/tccon.ggg2014.documentation.r0/1221662, 2015.

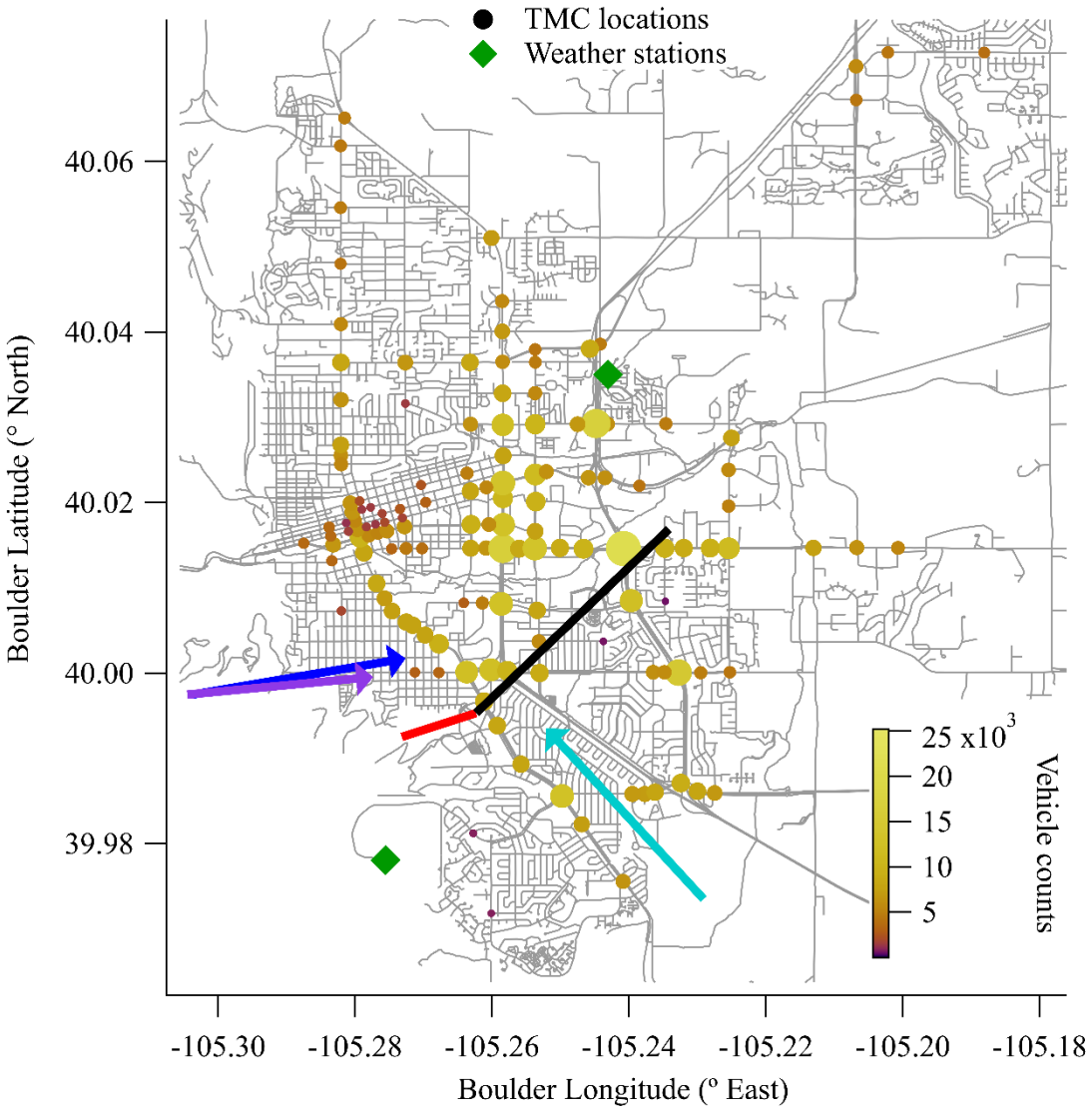

Figure 1: Measurement layout. The two measurement paths are shown by red (reference) and ~~blue~~ black (over-city) lines. The two weather stations that provided wind speed and direction data are given by the ~~sun symbols~~green diamonds. The ~~green markers~~colored circles are Turning Movement Count (TMC) locations, which are used as a proxy for the traffic ~~and the Gaussian plume s~~source locations. Both color and size represent the number of traffic counts at each location. Dominant wind directions for the campaign overall (aqua) and the test case days (purple for 10/22 and blue for 10/25) are given by colored arrows. ~~Data: Google, USDA, USGS, Digital Glob~~

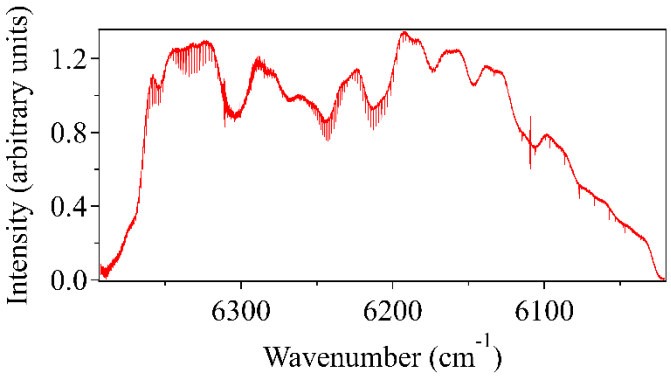

Figure 2~~2~~: Typical 32-second spectrum measured over the 2-km reference path. CO_2 bands are observed in the 6350 cm^{-1} and 6225 cm^{-1} regions, while CH_4 and H_2O are measured between 6150 and 6050 cm^{-1}. The larger, slowly varying structure is from the comb ~~spectra~~intensity profile. The atmospheric absorption appears as the small and narrow dips.

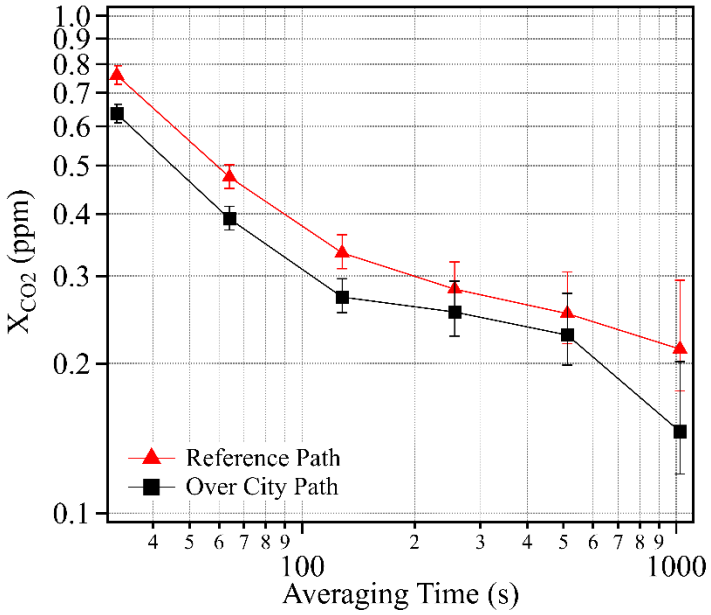

Figure 3: Statistical uncertainty as quantified by the Allan deviations for X_{CO2} over both the reference path (red triangles) and city path (black squares) from ~~during~~ a well-mixed, ~~flat~~ three-hour ~~measurement~~ time period on the night of October 3, 2016.

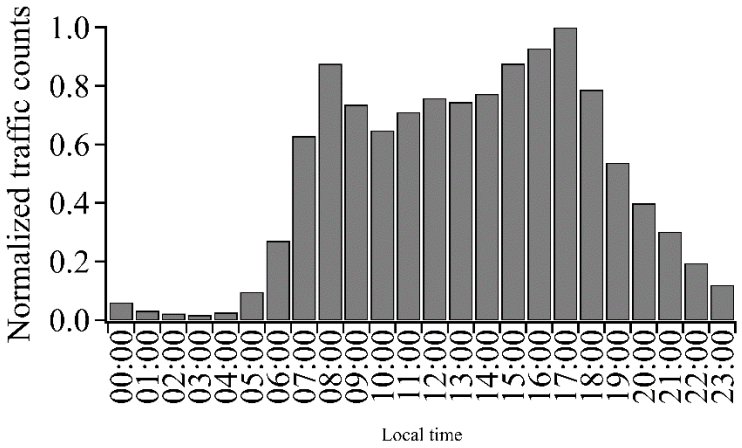

Figure ~~43~~ 42: City-wide traffic counts from the Boulder Arterial Count Program (ART), normalized to a peak of unity.

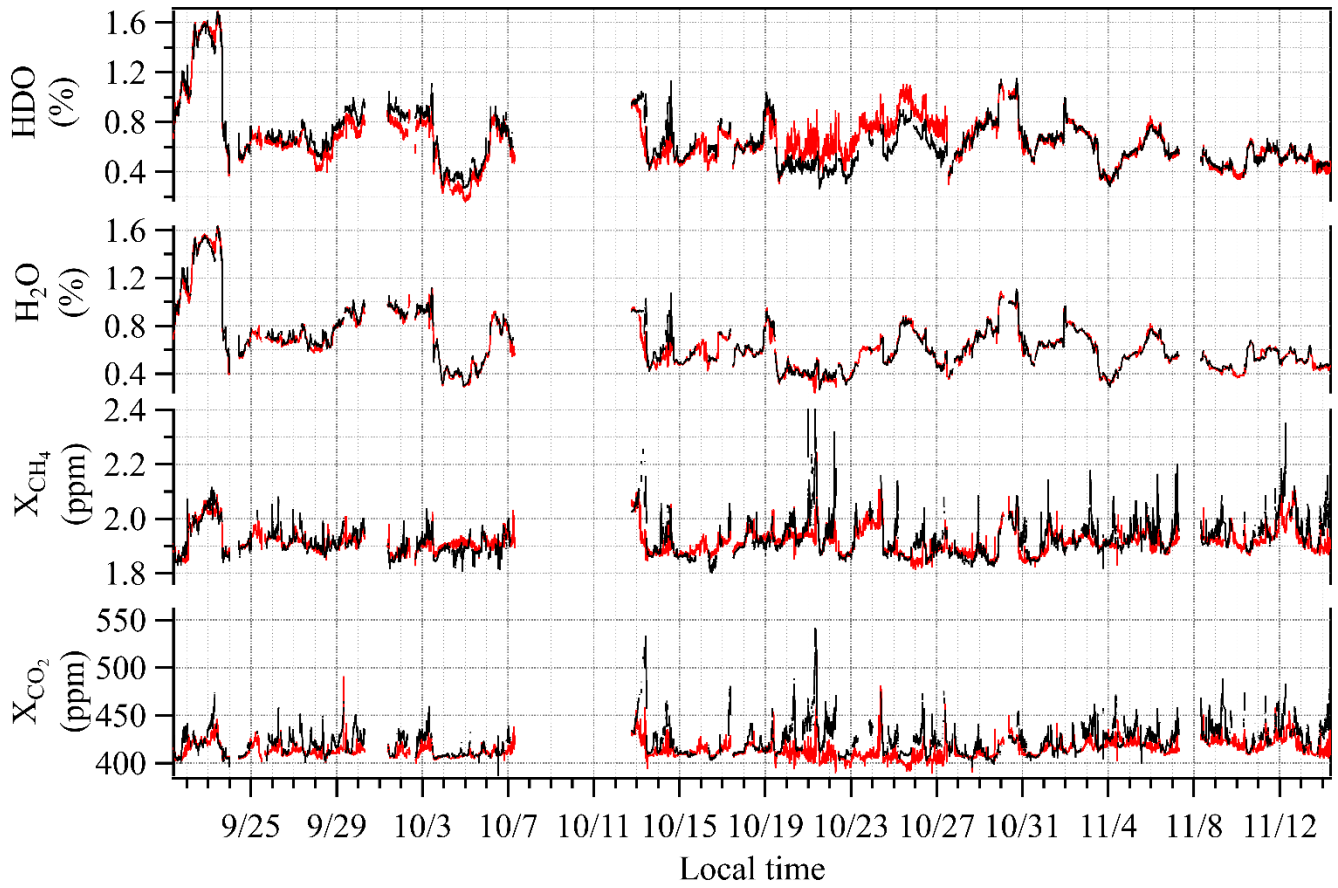

Figure 54: 7.5 weeks of dual-comb spectroscopy data for the reference path (red) and the over-city path (black) smoothed to 5-minute~~at 30-second~~ time intervals. Enhancements in the over-city path relative to the reference path are observed in CO_2 and CH_4 but not in H_2O or HDO. (Note: the HDO concentration includes the HITRAN isotopic scaling.)

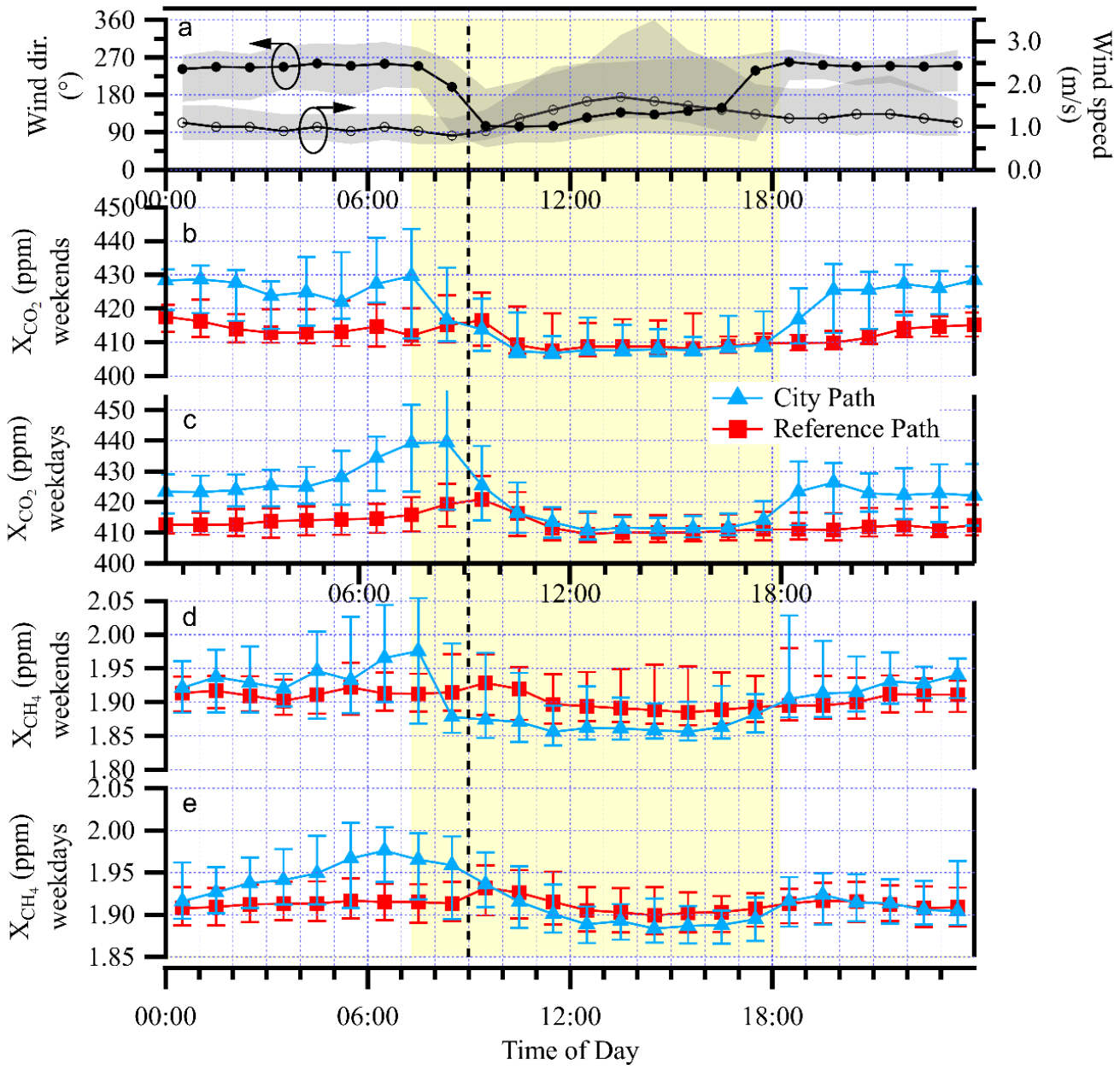

Figure 6~~5~~: Diurnal cycle analysis. Data is the median of the full 7.5 weeks. (a) The mean direction in which the wind is blowing ~~direction as measured from its origin~~ (black trace, left axis) and wind speed (gray trace, right axis) both from the NCAR Foothills measurement station, shaded regions reflect the 25th to 75th quartiles; (b) the weekend and (c) weekday median X_{CO2} ~~over the city path (light grey dots) and reference path (dark gray dots) over all days as well as median~~ values for the over-city path (blue triangles) and reference path (red squares). Uncertainty bars represent the 25%-75% range of values encountered. (d) and (e) Same data for X_{CH4}. The vertical dashed black line marks 9:00 local time and the yellow shaded region highlights the region from sunrise to sunset on Oct. 22, 2016.

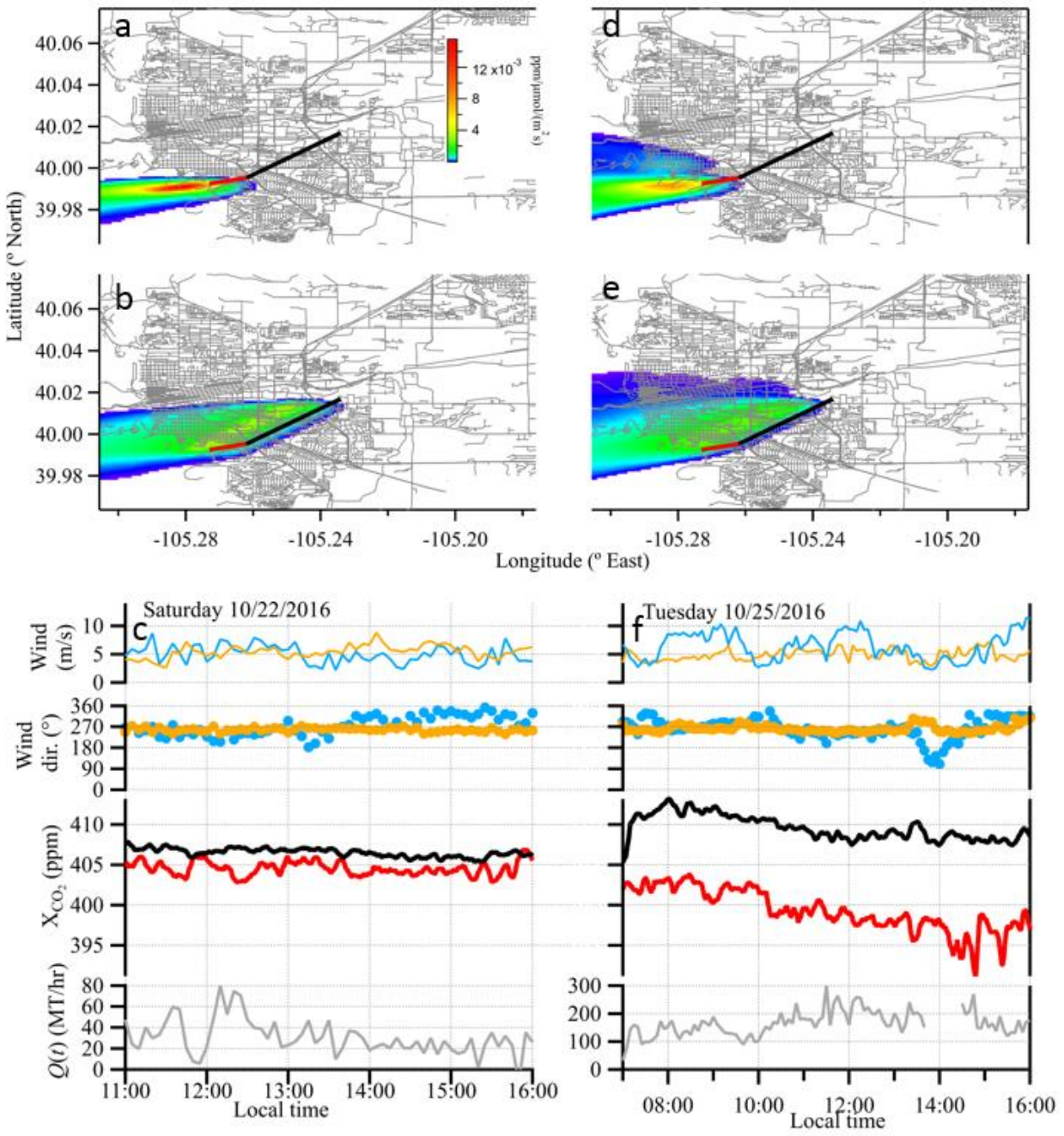
a
b
d
e
c
f
Latitude (° North)
Longitude (° East)
40.06
40.04
40.02
40.00
39.98
-105.28
-105.24
-105.20
12 x10^-3
8
4
ppm/(mol/(m s))
Saturday 10/22/2016
Tuesday 10/25/2016
Wind (m/s)
Wind dir. (°)
X_CO2 (ppm)
Q(t) (MT/hr)
Local time
11:00
12:00
13:00
14:00
15:00
16:00
08:00
10:00

1444

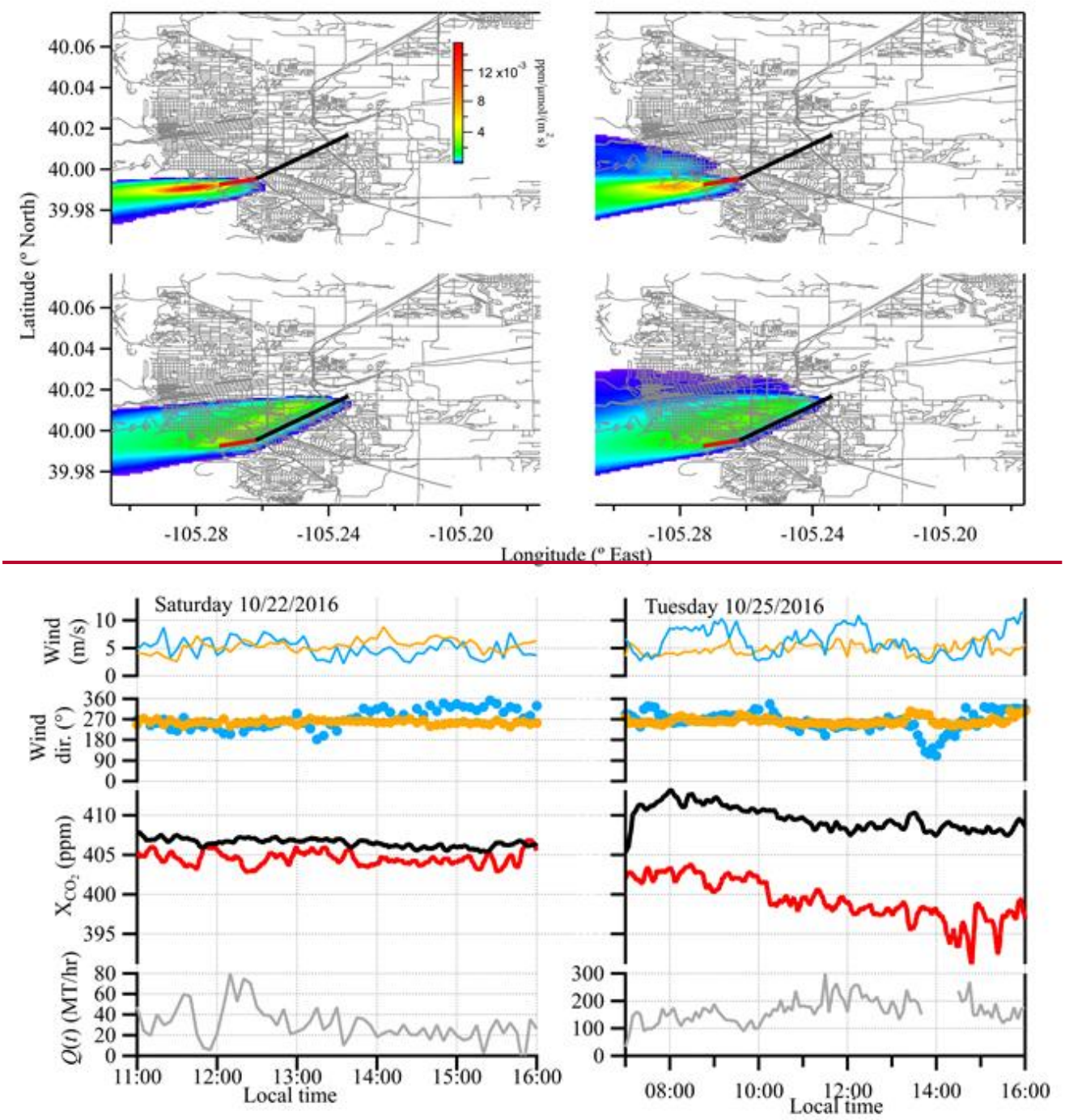

Figure 7~~6~~: Footprint calculations and ~~T~~time series data for the two case study days. Left column: Saturday, October 22, 2016; right column: Tuesday, October 25, 2016 data. Upper panels (a, d): Footprints for the reference path. Middle panels (b, e): Footprints for the over-city path. The footprints are averaged over the respective time windows and open paths. Lower panels (c,f): Wind and CO_2 data at ~~30 second~~5-minute time intervals. ~~Left plot: Saturday, 22 Oct. 2016. Right plot: Tuesday, 25 Oct. 2016.~~ Reference and over-city measurement paths are shown ~~in a, b, d, and e~~ in red and black, respectively. Data plots ~~Figures~~ show X_{CO2} ~~and X_{CH4}~~ over the reference path (red) and city path (black), ~~as well as~~ wind speed and wind direction measurements taken at NCAR Mesa (blue) and NCAR Foothills (orange), and the calculated ~~. Bottom panel in each plot shows~~ $Q(t)$ ~~for each day~~. On Oct. 25, ~~-~~$Q(t)$ data near 14:00~~-~~ has been removed since the

reference path wind directionn ~~(NCAR Mesa)~~ is out of the southeast to east, resulting in city contamination along the reference path. All data is smoothed to 5-minute time intervals.

Table I: Parameters used to calculate the emission rate from Eq. (4). The measurement precision refers to the instrument uncertainty in the measurement quantity. The variability refers to the observed environmental variability over the measurement period. The variability from the enhancement, the wind direction, and the wind speed drive the observed variability in the estimated $Q(t)$ ~~$Q(t)$~~ . (The distance from a given source location to the DCS measurement path, Δx_j ~~Δx_j~~, varies with location and has a 5-m uncertainty.)

		10/22 11:00-16:00		10/25 ~~10~~7:00-16:00	
Quantity	Measurement precision	Mean	Variability	Mean	Variability
Pathlength L ~~L~~	0.15 m	6730.66 m	0	6730.66 m	0
Enhancement (c-c_0)	0.28~~9~~ ppm (ref.) 0.2~~5~~ ppm (city)	1.9~~98~~ ppm	0.97~~1.4~~ ppm (49~~72~~%)	10.3~~9~~ ppm	1.92~~.3~~ ppm (192~~1~~%)
Wind speed u ~~u~~	0.3 m/s	5.2 m/s	1~~0~~.0~~85~~ m/s (19~~6~~%)	5.6 m/s	1.3~~4~~ m/s (23~~5~~%)
Solar insolation	5%	570 W/m^2	76 W/m^2 (13%)	275 W/m^2	185 W/m^2 (67%)
Wind direction ϕ ~~θ~~	2°	265°	21~~0~~°	26~~41~~°	15~~27~~°